An intestinally secreted host factor limits bacterial colonization but promotes microsporidia invasion of *C. elegans*

Hala Tamim El Jarkass[1], Calvin Mok[1], Michael R. Schertzberg[3], Andrew G. Fraser[1,3], Emily R. Troemel[2], Aaron W. Reinke[1#].

[1] Department of Molecular Genetics, University of Toronto, Toronto, ON, Canada.

[2] Division of Biological Sciences, University of California, San Diego, La Jolla, California, United States of America.

[3] Donnelly Centre, University of Toronto, Toronto, ON, Canada

#Corresponding author

aaron.reinke@utoronto.ca

Abstract

Microsporidia are ubiquitous obligate intracellular pathogens of animals. These parasites often infect hosts through an oral route, but little is known about the function of host intestinal proteins that facilitate microsporidia invasion. To identify such factors necessary for infection by *Nematocida parisii*, a natural microsporidian pathogen of *Caenorhabditis elegans*, we performed a forward genetic screen to identify mutant animals that have a Fitness Advantage with *Nematocida* (Fawn). We isolated four *fawn* mutants that are resistant to *Nematocida* infection and contain mutations in *T14E8.4*, which we renamed *aaim-1* (Antibacterial and Aids invasion by Microsporidia). Expression of AAIM-1 in the intestine of *aaim-1* animals restores *N. parisii*

infectivity and this rescue of infectivity is dependent upon AAIM-1 secretion. *N. parisii* spores in *aaim-1* animals are improperly oriented in the intestinal lumen, leading to reduced levels of parasite invasion. Conversely, *aaim-1* mutants display both increased colonization and susceptibility to the bacterial pathogen *Pseudomonas aeruginosa* and overexpression of *AAIM-1* reduces *P. aeruginosa* colonization. Competitive fitness assays show that *aaim-1* mutants are favoured in the presence of *N. parisii* but disadvantaged on *P. aeruginosa* compared to wild type animals. Together, this work demonstrates how microsporidia exploits an antibacterial immune protein to promote host invasion. Our results also highlight the evolutionary trade-offs that exist to optimizing host defense against multiple classes of pathogens.

Introduction

Microsporidia are a large group of obligate intracellular parasites that infect most types of animals.[1] These ubiquitous parasites possess the smallest known eukaryotic genome size, and are extremely reliant on their host as a result of the loss of many genes involved in metabolism and energy production.[2,3] Microsporidia can have a large impact on the evolution of their hosts, as infection with microsporidia often leads to a reduction in host offspring and the effect of this selective pressure has resulted in resistant animals within a population.[4,5] Microsporidia are currently a major threat to many commercially important species such as honeybees and shrimp.[6,7] Many species also infect humans and infections in immunocompromised individuals can result in lethality.[8] Despite their ubiquitous nature, effective treatment strategies are currently lacking for these poorly understood parasites.[9]

Microsporidia infection begins with invasion of host cells. They possess the most fascinating invasion machinery, a unique structure known as the polar tube.[10] This apparatus, resembling a long thread, is often coiled within a dormant spore. However, once inside of a host, and in proximity to the tissue of interest, the polar tube rapidly emerges or "fires" , releasing its the parasites infectious material (the sporoplasm) which is deposited intracellularly either through direct injection, or through the internalization of the sporoplasm.[10,11]

A number of microsporidia proteins have been demonstrated to play important roles during invasion by insect- and human-infecting species of microsporidia.[10] For example, spore wall proteins can interact with host cells through the recognition of sulfated glycosaminoglycans, heparin binding motifs, integrins, and proteins on the cell surface. [12–17] In *Encephalitozoon* species polar tube proteins (PTP) can mediate interactions with the host. For instance, O-linked mannosylation on PTP1 has been demonstrated to bind mannose binding receptors, whereas PTP4 interacts with the transferrin receptor (Trf1).[11,18–20] Additionally, the sporoplasm surface protein, EhSSP1, binds to an unknown receptor on the cell surface.[21] These proteins on the spore, polar tube, and sporoplasm have all been shown to promote microsporidia adhesion or invasion of host cells in culture systems, but the role of these proteins during animal infection is unclear.

The nematode *Caenorhabditis elegans* is infected in its natural habitat by several species of microsporidia, and frequently by *Nematocida parisii.*[22–24] This species infects the intestinal cells of *C. elegans,* which possess extreme similarity to those of mammalian cells, making it both a relevant tissue and model to study these infections in vivo.[24,25] Infection of *C. elegans* by *N. parisii* begins when spores are consumed by the worm, where they then pass through the pharynx into the

intestinal lumen and fire, depositing sporoplasms inside of intestinal cells. Within 72 hours the sporoplasm will divide into meronts, which differentiate into spores, that then exit the animal, completing the parasite's life cycle.[26,27] Infection with *N. parisii* leads to reduced fecundity and premature mortality[24,26] Several mutants have been shown to affect proliferation and spore exit.[28,29] Immunity that can either prevent infection or clear the pathogen once infected have also been described.[4,27,30–32] In contrast, very little is known about how *N. parisii* invades *C. elegans* intestinal cells. Almost all of the microsporidia proteins known to facilitate invasion are not conserved in *N. parisii* and although host invasion factors described in other species are present in *C. elegans*, there is no evidence that they are being used by microsporidia during invasion of *C. elegans.*[11]

To understand how microsporidia invade animal cells, we performed a forward genetic screen to identify host factors that promote infection. We identified a novel, nematode-specific protein, AAIM-1, whose loss of function confers resistance to microsporidia infection. This protein is expressed in intestinal cells, secreted into the intestinal lumen, and is necessary to ensure proper spore orientation during intestinal cell invasion. In addition, we show that AAIM-1 limits bacterial colonization of pathogenic *Pseudomonas aeruginosa*. Strikingly, T14E8.4 plays opposing roles on host fitness in the face of pathogenesis. The utilization of a host factor critical for bacterial defense reflects a clever strategy to ensuring microsporidia's reproductive success.

Results

A forward genetic screen identifies *aaim-1* as being necessary for *N. parisii* infection.

92 To identify host factors needed for infection by microsporidia, we carried out a forward genetic
93 screen using a *C. elegans* model of *N. parisii* infection. We took advantage of the previously
94 described phenotypes of *C. elegans* displaying reduced fitness when infected with *N. parisii,*
95 including lower progeny production and stunted development.[26,27,33] We mutagenized animals and
96 subjected F2 progeny to *N. parisii* infection. After infecting populations for five subsequent
97 generations, we selected individual worms containing embryos, indicating increased fitness in the
98 presence of infection (see Methods). We identified four independent isolates that reproducibly had
99 higher fractions of animals containing embryos compared to wild type (N2). We named these
100 isolates Fitness Advantage With *Nematocida* (*fawn* 1-4) (Figure S1a).
101
102 We first determined if these *fawn* mutants were also resistant to *N. parisii* infection. We grew the
103 three isolates with the strongest phenotype, *fawn* 1-3, in the presence and absence of *N. parisii*,
104 and stained each population of worms with the chitin binding dye, Direct-yellow 96 (DY96), at 72
105 hours post infection (hpi). DY96 allows for the visualization of chitinous microsporidia spores as
106 well as worm embryos (Figure 1a). In the absence of infection, there is no difference in the fraction
107 of *fawn-2* and *fawn-3* animals developing into adults containing embryos (gravid adults), although
108 *fawn-1* has a modest defect. In comparison, all three *fawn* isolates generate significantly more
109 gravid adults than N2 animals in the presence of infection (Figure 1b). We next examined the
110 fraction of animals in each strain containing intracellular microsporidia spores and observed that
111 all three *fawn* isolates display significantly fewer numbers of spore-containing worms (Figure 1c).
112 These results suggest that *fawn* mutants are missing an important factor for efficient microsporidia
113 infection.
114

To identify the causal mutations underlying the Fawn phenotype, we used a combination of whole-genome sequencing and genetic mapping. We generated F2 recombinants and performed two rounds of infection with microsporidia, selecting for gravid animals. After each round we used molecular inversion probes to determine the region of the genome linked to the causal mutation.[34] This revealed strong signatures of selection on the left arm of chromosome X in all three *fawn* isolates absent in N2 (Figure S1b). Analysis of whole genome sequencing showed that all four *fawn* isolates contained different alleles of *T14E8.4*, which we named *aaim-1* (Antibacterial and Aids Invasion by Microsporidia-1) for reasons described below (Figure 1d). We validated the role of *aaim-1* in resistance to infection using several additional alleles: an independent allele RB563 (*ok295*), carrying a large gene deletion in both *aaim-1* and *dop-3,* and a CRISPR-Cas9 derived allele, *aaim-1 (kea22),* that contains a large gene deletion. Both of these alleles displayed a fitness advantage when infected with *N. parisii* (Figure 1d,e, S1c,d). These data demonstrate that *aaim-1* is the causative gene underlying the *fawn* 1-4 infection phenotypes. In subsequent experiments we utilized both *aaim-1 (kea22)*, and *fawn-3 (kea28),* carrying a 2.2 kb deletion in *aaim-1,* which was outcrossed to N2 six times.

aaim-1 is expressed in the pharynx and intestine, and secretion is important for function.

AAIM-1 is a poorly characterized protein that does not possess any known or conserved domains. Homologs of the protein exist in both free-living and parasitic nematodes (Figure S2). To further characterize the role of AAIM-1 during *N. parisii* infection, we generated transgenic extrachromosomal lines of *C. elegans* carrying a reporter strain of GFP under control of the *aaim-1* promoter. GFP fluorescence was observed in the terminal bulb of the pharynx as well as the

137 posterior of the intestine throughout development (Figure 2a). Embryos and L1 animals display
138 additional expression in the arcade cells of the pharynx (Figure 2a, S3a).
139
140 The first 17 amino acids of AAIM-1 are predicted to encode a signal peptide.[35] This suggests that
141 AAIM-1 may be secreted into the pharyngeal and intestinal lumen, the extracellular space through
142 which *N. parisii* spores pass before invading intestinal cells. To test where AAIM-1 functions in
143 and if secretion is important for function, we generated a series of transgenic worms expressing
144 extrachromosomal arrays (Supplemental table 1). First, we generated transgenic *aaim-1 (kea22)*
145 animals expressing AAIM-1 tagged on the C-terminus with a 3x Flag epitope. Transgenic animals
146 expressing AAIM-1 under its native promoter complement the ability of *aaim-1 (kea22)* animals
147 to develop into adults in the presence of a high amount of *N. parisii* spores (Figure 2b). A construct
148 expressing GFP or GFP::3xFlag does not influence this phenotype nor does the presence of the
149 epitope tag impair the ability of AAIM-1 to rescue the mutant phenotype (Figure S3b). We next
150 generated a signal peptide mutant allele of AAIM-1 missing the first 17 amino acids *(SPΔaaim-*
151 *1),* which is unable to complement the *aaim-1 N. parisii* infection phenotype. In contrast, AAIM-
152 1 expressed from an intestinal specific promoter can rescue the infection phenotype of *aaim-1*
153 *(kea22)* (Figure 2b).
154
155 To determine where AAIM-1 localizes, we dissected the intestines from transgenic worms and
156 performed immunofluorescence using anti-Flag antibodies. We were unable to detect expression
157 of AAIM-1::3xFlag when expressed from its endogenous promoter. However, we observed protein
158 expression in the intestinal cells of animals expressing AAIM-1::3xFlag from a strong, intestinal
159 specific promoter or when the signal peptide was removed (Figure 2c).[36] We did not observe

AAIM-1::3xFlag localized in the extracellular space of the intestinal lumen, possibly due to rapid turnover of intestinal contents or due to loss from dissection of the intestines.[37] The increased expression in the signal peptide mutant suggests an accumulation of protein that is unable to be secreted. Taken together, these data demonstrate that AAIM-1 is secreted and acts within the intestinal lumen to promote *N. parisii* infection.

AAIM-1 is only necessary for microsporidia infection at the earliest larval stage.

N. parisii infection of *C. elegans* can occur throughout development, but several forms of immunity towards microsporidia have been shown to be developmentally regulated.[4,27] To determine if *aaim-1* mutant animals display developmentally restricted resistance to infection, we infected *fawn* 1-3 at the L1 and L3 stage. For these experiments we took advantage of another intestinal-infecting species of microsporidia, *Nematocida ausubeli*, which has a more severe effect on *C. elegans* fecundity, allowing us to determine fitness defects after the L1 stage.[4,23,26] *fawn* isolates are resistant to *N. ausubeli* as seen by an increase in the fraction of gravid adults in the population after exposure to a medium dose of *N. ausubeli* (Figure 3a). When we initiated infections at the L3 stage of growth, *fawn* isolates do not have increased resistance, and instead exhibit wild type levels of susceptibility (Figure 3b). To rule out the possibility that this L1 restricted phenotype was the result of exposure to sodium hypochlorite treatment, used to synchronize worms, we exposed embryos that were naturally laid by adults within a two-hour window to *N parisii* infection. Animals synchronized in this manner still display a robust resistance to *N. parisii* (Figure S4c). Thus, resistance to infection in *aaim-1* mutants is developmentally restricted and AAIM-1 is utilized by multiple different species of microsporidia.

AAIM-1 is needed for efficient invasion of intestinal cells

Resistance to infection could be the result of a block in invasion, proliferation, or through the destruction of the parasite. To test the mechanism of resistance in *aaim-1* mutants, we performed pulse-chase infection assays at the L1 and L3 stage of development.[4,27] Here, we treated animals with a medium-1 dose of *N. parisii* for 3 hours, washed away any un-ingested spores, and then replated the animals in the absence of spores for an additional 21 hours. We then used an 18S RNA FISH probe to detect *N. parisii* sporoplasms, which is the earliest stage of microsporidia invasion. In our *fawn* 1-3 isolates we detect less invasion at 3hpi compared to N2 (Figure S4a). However, there was no reduction in the number of infected animals between 3hpi and 21 hpi, indicating that pathogen clearance was not occurring. This defect in invasion was not present at the L3 stage, providing further support that resistance is restricted to the L1 stage in *aaim-1* mutants (Figure S4b). A reduction in invasion could be due to a feeding defect, leading to a reduction in spore consumption. To test rates of consumption, we measured the intestinal accumulation of fluorescent beads. We find that *aaim-1* alleles displayed wild-type levels of bead accumulation, unlike the feeding defective strain *eat-2 (ad465)* (Figure S4d).

For *N. parisii* to invade host cells, spores must first enter the intestinal lumen and fire their polar tube.[27] To test if *aaim-1* mutants have defects in spore entry or spore firing, we infected animals for either 45 minutes or 3 hours, at the L1 and L3 stages. We then fixed and stained animals with both *N. parisii* 18S RNA FISH probe and DY96 and quantified the number of spores present in the intestinal lumen of animals. Here, *aaim-1* animals infected for 45 minutes or 3 hours at L1 or L3 contained similar amounts of spores as N2 animals (Figure 3 c,f, S5a,d). The percentage of fired spores present within these animals is also not significantly different at either developmental

stage (Figure 3d,g, S5b,e). We then counted the number of sporoplasms per animal and observed significantly fewer invasion events in *aaim-1* mutant animals infected at L1 (Figure 3e, S5c). In contrast the number of sporoplasms in L3 stage *aaim-1* alleles are similar to that observed in the N2 strain (Figure 3h, S5f). These results demonstrate that the *N. parisii* invasion defect in *aaim-1* mutants is not caused by differences in spore firing or accumulation. Instead, these results suggest that spores are misfiring, leading to unsuccessful invasion.

AAIM-1 plays a role in promoting proper spore orientation

To determine how AAIM-1 promotes *N. parisii* invasion, we further examined the invasion process. We pre-stained spores with Calcofluor white (CFW) and assessed their orientation relative to the intestinal apical membrane in L1 worms infected for 45 minutes (Figure 4a). In N2 animals, 32.4% of spores are angled relative to the apical membrane. In contrast, spores in *aaim-1* alleles were angled 14.3% of the time (Figure 4b). Other host factors that promote microsporidia invasion cause adherence to host cells.[11] To determine if AAIM-1 influences the location of spores relative to intestinal cells in *aaim-1* mutants, we measured the perpendicular distance from the center of a parallel spore to the apical membrane of the intestine. Surprisingly, parallel spores in *aaim-1* alleles were significantly closer to the apical membrane (0.29 μm) than those in N2 (0.34 μm) (Figure 4c). In agreement with resistance being developmentally restricted, *aaim-1* mutants display wild-type spore orientations and distances from the membrane when infections were initiated at L3 (Figure 4d,e). The width of the intestinal lumen at L1 does not differ significantly between N2 and *aaim-1* mutants, however, L3 animals generally possess wider intestinal lumens (Figure S5g,h). Thus, taken together these results suggest that AAIM-1 plays a distinct role in the intestinal

lumen at L1 to promote proper spore orientation, through maintaining an appropriate distance and angle to the apical membrane, resulting in successful invasion.

AAIM-1 inhibits intestinal colonization by *Pseudomonas aeruginosa*

Interestingly, *aaim-1* has been shown to be upregulated by a variety of different fungal and bacterial pathogens, including *P. aeruginosa*. [38,39] Using our transcriptional reporter strain, we sought to confirm this and determine if microsporidia infection could also induce *aaim-1* transcription. N2 animals carrying a transcriptional reporter (p*aaim-1*::GFP::3xFlag) were exposed to *N. parisii, P. aeruginosa* PA14, or *E. coli* OP50, and the levels of GFP quantified when grown on these pathogens for 72 hours from the L1 stage, or for 24 hours from the L4 stage. Infection by either *N. parisii* or *P. aeruginosa* PA14 resulted in the upregulation of *aaim-1* as detected by an increase in the GFP signal (Figure 5a, S6e).

Previously, an *aaim-1* deletion strain, RB563 *(ok295),* was shown to display reduced survival on lawns of *P. aeruginosa* PA14.[40] The enhanced susceptibility previously reported was attributed to *dop-3,* which is also partially deleted in RB563 *(ok295)*. [40] To determine if *aaim-1* mutants are susceptible to pathogenic bacterial infection, we assayed the survival of L4 stage worms in *P. aeruginosa* PA14 slow killing assays was quantified. Here, *aaim-1* alleles displayed reduced survival compared to N2, indicating that *aaim-1* mutants have enhanced susceptibility to PA14 (Figure 5b, S6a,b).

Lethality in slow killing assays is a result of *P. aeruginosa* accumulation within the intestinal lumen.[41,42] To investigate if *aaim-1* alleles displayed higher levels of bacterial burden, animals

grown on lawns of PA14::DsRed at the L1 or L4 stage for 48 hours. *aaim-1* mutant alleles grown on lawns of PA14::DsRed as L4s, but not L1s, displayed higher bacterial burden relative to N2 (Figure 5c, S6c,d). To test if intestinal expression of *aaim-1* was sufficient to limit bacterial colonization, transgenic *aaim-1 (kea22)* overexpressing AAIM-1::3xFlag from the endogenous or an intestinal specific (*spp-5)* promoter were exposed to lawns of PA14::DsRed. When grown for 48 hours at the L1 or L4 stage, bacterial burden was significantly reduced, relative to N2 (Figure 5d, e). The results indicate that AAIM-1 plays a role in limiting bacterial colonization, and its loss results in reduced survival due to hyper-colonization of the intestinal lumen.

Fitness of *aaim-1* animals is dependent upon microbial environment

To investigate how *aaim-1* alleles can influence population structure, we set up competitive fitness assays. A *C. elegans* strain with a fluorescent marker (RFP::ZNFX1) was co-plated with N2 or *aaim-1* mutants on *E. coli* OP50, *N. parisii* or *P. aeruginosa* PA14. Animals were grown for 8 days, such that the population was composed of adult F1s and developing F2s. On *E. coli* OP50, there is equal representation of N2 and *aaim-1* mutants in the population (Figure 6a). This is consistent with *aaim-1* mutants not having a developmental delay (Figure 1b) or a decrease in longevity (Figure S7). In contrast, growth on *N. parisii* resulted in *aaim-1* alleles outcompeting the N2 strain. Conversley, *aaim-1* mutants on *P. aeruginosa* PA14 did significantly worse, being underrepresented in the population compared to N2 (Figure 6a). Interestingly, wild isolates of *C. elegans* do not carry any obvious loss of function alleles of *aaim-1* suggesting that natural conditions have selected for its retention (Figure S8). [43]

Given the opposing fates of *aaim-1* mutants on *N. parisii* and *P. aeruginosa,* we investigated the effects of co-infection. Animals were infected with a maximal dose of *N. parisii* for 3 hours, prior to placement on lawns of PA14. For infections with a single pathogen, we observed similar results as before whereby *aaim-1* mutants have increased fitness in the presence of *N. parisii* and display lower levels of parasite burden but have increased bacterial accumulation when grown on PA14. In the presence of both pathogens, populations of *aaim-1* mutants display fewer gravid adults and increased amounts of *N. parisii* spores. (Figure 6b,c). These results suggests that coinfection with *N. parisii* and *P. aeruginosa* has synergistically negative effects on the fitness of *C. elegans*.

Discussion:

To identify host factors needed for microsporidia infection, we isolated mutants from a forward genetic screen that have a fitness advantage when challenged with *N. parisii* infection. This screen identified mutants in the poorly understood protein AAIM-1 (previously T14E8.4). Here, we demonstrate that this protein both promotes microsporidia invasion and limits colonization by pathogenic bacteria. Although we were unable to visualize the localization of secreted AAIM-1, our genetic and infection experiments strongly suggest that this protein acts in the intestinal lumen where both microsporidia invasion and bacterial colonization both take place. The key role that AAIM-1 plays in immunity is further exemplified by its transcriptional regulation in response to infection (Figure 7).

The processes by which microsporidia invade host cells are poorly understood. We show that *N. parisii* spores are often angled in wild-type *C. elegans*, suggesting that successful invasion requires a particular spore orientation. In the absence of AAIM-1, spores are more often parallel to the

intestinal lumen, where spores may fire without the successful deposition of the sporoplasm inside an intestinal cell. In contrast to previously described host and microsporidia proteins involved in invasion, AAIM-1 does not appear to be involved in promoting adhesion to the surface of host cells.[10,11] Instead, AAIM-1 ensures an adequate distance of spores from the intestinal membrane, possibly allowing spores to be able to properly orient themselves to ensure proper host cell invasion. *N. parisii* spores are ~2.2 μm long by ~0.8 μm wide and the average width of the intestinal lumen at the L1 stage is ~0.6 μm[23]. Therefore, at the L1 stage spores may not be able to move freely, but at the L3 stage, where AAIM-1 is not needed for invasion, there is less of a constraint on spore movement as the luminal width increases to ~1.3 μm. Together, our results highlight the power of studying microsporidia invasion in the context of a whole animal model.

C. elegans employs a variety of proteins to protect against bacterial infection. Many of these proteins belong to several classes of antimicrobial effectors used to eliminate and prevent colonization by pathogenic bacteria[44], are upregulated upon infection and predicted to be secreted.[45,46] One class of secreted proteins that are known to have immune functions and prevent bacterial adherence are the mucins. These large, glycosylated secreted proteins are upregulated during *C. elegans* infection and their knockdown alters susceptibility to *P. aeruginosa* infection.[47,48] AAIM-1 has many predicted mucin-like O-glycosylation sites on serine and threonine residues.[49–51] Thus one possibility is that AAIM-1 may be functionally analogous to mucins, preventing the adhesion of microbes to the surface of intestinal cells. As AAIM-1 does not contain any known or conserved domains and further work will be necessary to determine its exact biochemical function.

C. elegans lives in a microbially dense environment containing a wide variety pathogens that *C. elegans* has evolved immunity towards.[23,52–55] Although loss of *aaim-1* provides a fitness advantage to *C. elegans* when grown in the presence of microsporidia, obvious loss of function alleles are not present in wild isolates sequenced thus far. Additionally, *aaim-1* mutants do not have observable defects when grown on non-pathogenic *E. coli*. This is in contrast to mutations in *pals-22* or *lin-35*, which negatively regulate the transcriptional response to infection and provide resistance to microsporidia infection when mutated, but at the cost of reduced reproductive fitness[27,56]. Loss of *aaim-1* disadvantages *C. elegans* when grown on *P. aeruginosa*, demonstrating that there is a trade-off in host defense between microsporidia and pathogenic bacteria. The opposing functions of *aaim-1* with different pathogens adds to the limited set of known examples of trade-offs that constrain the evolution of host defense to multiple biotic threats[57,58]

Methods

Strain maintenance

C. elegans strains were grown at 21°C on nematode growth media (NGM) plates seeded with 10x saturated *Escherichia coli* OP50-1.[27] Strains used in this study are listed in Supplemental table 1. For all infection assays, 15-20 L4 staged animals were picked onto 10cm seeded NGM plates 4 days prior to sodium hypchlorite/1M NaOH treatment. After 4 days, heavily populated non-starved plates were washed off with 1ml M9, treated twice with 1 ml of sodium hypochlorite/1M NaOH solution, and washed three times in 1 ml M9. Embryos were then resuspended in 5 ml of M9 and left to rock overnight at 21°C. L1's were used in subsequent experiments no later than 20 hours

after bleach treatment. All centrifugation steps with live animals/embryos were performed in microcentrifuge tubes at 845xg for 30s.

Throughout the paper, L1 refers to the stage immediately post hatching or bleach synchronization, L3 refers to 24 hours and L4 refers to 48 hours post plating of bleach synchronized L1's at 21°C. L3 and L4 animals were washed off plates in M9 + 0.1% Tween-20, followed by an additional wash to remove residual bacteria before infection with microsporidia, or plating on PA14.

Forward Genetic Screen

6,000 L4 N2 hermaphrodites were mutagenized with a combination of 50 mM EMS and 85.4 mM ENU for 4 hours to achieve a large diversity of mutations within the genome.[59] P0 animals were then split and placed onto 48 10cm NGM plates, F1s bleached and resulting F2s pooled onto 5 separate plates. 180,000 L1 F2 animals were plated onto a 10 cm plate with 10 million *N. parisii* spores and 1 ml 10x saturated OP50-1. Animals were grown for 72 hours, to select for animals that display a fitness advantage phenotype with respect to N2. Each population was bleached and grown in the absence of infection for one generation, in order to prevent the effects of intergenerational immunity[27]. Two more cycles of infection followed by growing worms in the absence of infection was performed. Populations of bleached L1s were then infected with either 20 or 40 million spores and grown for 76 hours. Worms were then washed into 1.5 ml tube and 1 ml of stain solution (1x PBS/0.1% Tween-20/2.5 mg/ml DY96/1% SDS) was added. Samples were incubated with rotation for 3.5 hours and then washed 3 times with M9 + 0.1% Tween-20. Individual worms that had embryos, but not spores, were picked to individual plates. Each of the four *fawn* strains was isolated from a different mutant pool.

364

365 **Whole genome sequencing**

366 N2 and *fawn* isolates were each grown on a 10 cm plate until all *E. coli* was consumed. Each worm
367 was washed off with M9 and frozen at -80°C. DNA was extracted using Gentra puregene Tissue
368 Kit (QIAGEN). Samples were sequenced on an Illumina HiSeq 4000, using 100 base paired end
369 reads.

370

371 **MIP-Map**

372 Molecular inversion probes were used to map the underlying causal mutations in *fawn* isolates as
373 previously described.[34] Briefly, *fawn* hermaphrodites were crossed to males of the mapping strain
374 DM7448 (VC20019 Ex[*pmyo3::*YFP*])* hereafter referred to as VC20019. Next, 20 F1
375 hermaphrodite cross progeny, identified as those carrying *pmyo3*::YFP were isolated and allowed
376 to self. F2s were then bleached, and 2,500 L1s were exposed to a medium-2 dose of *N. parisii*
377 spores representing the first round of selection. Two plates of 2,500 F3 L1s were set up. The
378 experimental plate was grown in the absence of infection for one generation, to negate
379 intergenerational immunity.[27] A second plate of 2,500 L1s was allowed to grow to 72 hours and
380 then frozen in H_20 at -80°C, until used for genomic preparation. The selection and rest steps were
381 repeated once more, and a second frozen sample of worms was taken at the end of the mapping
382 experiment. This process was also performed for a cross between N2 hermaphrodites and males
383 of the mapping strain VC20019, as a negative control to identify non-causal loci that may be
384 selected for reasons other than resistance to infection. Two genomic preparations, corresponding
385 to the two rounds of selection, were used as template for MIP capture, to generate multiplexed
386 libraries for sequencing. An Illumina Mini-seq was used to generate sequencing data that was

subjected to demultiplexing via R, and selection intervals were defined as those immediately adjacent to the region on the chromosome carrying the fewest proportion of reads corresponding to the mapping strain, VC20019. This interval was then used to scan for putative causal alleles, resulting in the identification of the four *aaim-1* alleles in the four *fawn* isolates.

Identification of causal gene

Variants were identified using a BWA-GATK pipeline. Briefly, sequencing reads were checked for sequence quality using FastQC (http://www.bioinformatics.babraham.ac.uk/projects/fastqc/) and bases lower than a quality threshold of 30 were trimmed off with Trimmomatic using a sliding window of 4 bases and minimum length of 36 bases.[60] Reads were aligned to the *C. elegans* N2 reference genome (release W220) using BWA-mem.[61] Alignments were sorted by coordinate order and duplicate reads removed using Picard (https://github.com/broadinstitute/picard). Prior to variant calling, reads were processed in Genome Analysis Tool Kit (GATK) v3.8.1,[62] to perform indel realignment and base quality score recalibration using known *C. elegans* variants from dbSNP, build 138 (http://www.ncbi.nlm.nih.gov/SNP/). GATK HaplotypeCaller was used to call variants, and results were filtered for a phred-scaled Qscore > 30 and to remove common variants found previously in multiple independent studies. Finally, Annovar [63] was used to obtain a list of annotated exonic variants for each sequenced strain.

Microsporidia infection assays

N. parisii (ERTm1) spores were prepared as described previously.[27] All infections were carried out on 6-cm NGM plates, unless otherwise specified by spore dose (see Supplemental table 2), or experimental method. 1,000 bleach-synchronized L1s were added into a microcentrifuge tube

410 containing 400 µl of 10X *E. coli* OP50, and spores. After pipetting up and down, this mixture was
411 top plated onto an unseeded 6-cm NGM plate, and left to dry in a clean cabinet, prior to incubation
412 at 21°C for 72 hours. Infections set up on 3.5-cm plates used 160 µl of 10x *E. coli* OP50 and 400
413 L1's.
414
415 **Infection of embryos hatched on plates**
416 Twenty-five 72-hour old synchronized animals of each strain were picked onto 3.5-cm unseeded
417 NGM plates seeded with 16 µl of 10x *E. coli* OP50. Plates were incubated at 21°C for two hours.
418 Adults were then picked off, and a mixture of 144 µl of 10x *E. coli* OP50 and a low dose of *N.*
419 *parisii* spores were added to each plate. Animals were fixed and stained after 72 hours.
420
421 **Pulse-chase infection assay**
422 6,000 bleach synchronized animals were exposed to a medium-1 (Figure S4) or medium-3 (Figure
423 3) dose of spores, 10 µl of 10x *E. coli* OP50 in a total volume of 400 µl made up with M9. To
424 assay pathogen clearance 3 hpi, animals were washed off in 1 ml M9 + 0.1%Tween-20, and split
425 into two populations. The first was fixed with acetone to represent initial infectious load, while the
426 other half was washed twice in M9 + 0.1% Tween-20 to remove residual spores in the supernatant
427 and prevent additional infection from occurring. These washed worms were then plated on 6-cm
428 unseeded NGM plates with 40 µl 10x OP50, and 360 µl M9 and left to incubate at 21°C for 21
429 additional hours before fixation.
430
431 **Spore localization and firing assays**

Strains were infected as described for the pulse infection assays for either 45 minutes or 3 hours. Animals were then washed off plates, fixed, and stained with DY96 and *N. parisii* 18S RNA FISH probe. $FISH^{+}$ $DY96^{+}$ events represent unfired spores, $FISH^{-}$ $DY96^{+}$ events represent fired spores and $FISH^{+}$ $DY96^{-}$ events represent sporoplasms. Percentage of fired spores is defined as the number of $FISH^{-}$ $DY96^{+}$ events over the total number of spores.

To assess spore orientation, the localization of spores relative to the apical membrane of the apical intestine was measured in live anaesthetized animals. To determine if a spore was angled, straight lines were extended from both ends of the spore independently. If either of these two lines crossed the apical membrane, a spore was considered angled. If not, the spore was considered parallel. Distance of spores from the apical membrane was assessed by measuring perpendicular distance from the central edge of a parallel spore to the apical membrane. All measurements were performed on FIJI[64] using the angle tool or the straight line tool respectively, followed by the Analyze → measure option.

Intestinal lumen measurements

Measurements were performed on live anaesthetized worms used for spore localization assays (see above). The width of the lumen was determined by extending a straight line from the apical membrane on one end of the worm to that directly across on the other end, at the midpoint of the intestine, and the distance measured in FIJI, via the straight line tool followed by the Analyze → measure option.

Fixation

455 Worms were washed off infection plates with 700 µl M9 +0.1% Tween-20 and washed once in
456 1ml M9+0.1%Tween-20. All microsporidia infected samples were fixed in 700 µl of acetone for
457 2 minutes at room temperature prior to staining. All *P. aeruginosa* PA14::DsRed infected samples
458 were fixed in 500 µl of 4% paraformaldehyde (PFA) for 30 minutes at room temperature prior to
459 mounting on slides.
460
461 **Live imaging**
462 Animals were mounted on 2% Agarose pads in 10 µl of 25mM Sodium Azide. This technique was
463 used for spore localization assays, transcriptional reporter imaging, and assessing PA14::DsRed
464 colonization in transgenic animals.
465
466 **Chitin Staining**
467 The chitin binding dye Direct yellow 96 (DY96) was usesd to assess host fitness (gravidity) as
468 well as parasite burden. 500 µl of DY96 solution (1 x PBST, 0.1% SDS, 20 µg/ml DY96) was
469 added to washed worm pellets and left to rock for 20-30 minutes at room temperature. Worms
470 were then resuspended in 20 µl of EverBrite™ Mounting Medium (Biotium), and 10 µl mounted
471 on glass slides for imaging.
472
473 To prestain spores prior to infection, 0.5 µl of Calcofluor white solution (CFW) (Sigma- Aldrich
474 18909) was added per 50 µl of spores, pipetted up and down gently and left for 2 minutes at room
475 temperature prior to infection.
476
477 **Fluorescence in Situ hybridization-FISH**

To quantify the number of sporoplasms in *N. parisii* infected animals, the MicroB FISH probe (ctctcggcactccttcctg) labelling *N. parisii* 18S RNA was used. Animals were fixed in acetone, washed twice in 1 ml PBST, and once in 1 ml of hybridization buffer (0.01% SDS, 900 mM NaCl, 20 mM TRIS pH 8.0). Samples were then incubated overnight in the dark at 46 °C with 100 µl of hybridization buffer containing 5 ng/µl of the MicroB FISH probe conjugated to Cal Fluor 610 (LGC Biosearch Technologies). Samples were then washed in 1ml of wash buffer (Hybridization buffer + 5 mM EDTA), followed by incubation with 500 µl wash buffer at 46 °C in the dark. To visualize sporoplasms and spores simultaneously, the final incubation was replaced with 500 µl DY96 solution and incubated in the dark at room temperature prior to resuspension in 20 µl of EverBrite™ Mounting Medium (Biotium).

Microscopy and image quantification

All imaging was performed using an Axio Imager.M2 (Zeiss), except for images of the transcriptional reporter in Figure S6, which were generated using an Axio Zoom V.16 (Zeiss) at a magnification of 45.5x. Images were captured via Zen software and quantified under identical exposure times per experiment. Gravidity is defined as the presence of at least one embryo per worm, and animals were considered infected by 72 hours if clumps of spores were visible in the body of animals as seen by DY96. FISH-stained animals were considered infected if at least one sporoplasm was visible in intestinal cells.

To quantify fluorescence within animals (Pathogen burden, bead accumulation, GFP), regions of interest were used to outline every individual worm from anterior to posterior, unless otherwise specified in methods. Individual worm fluorescence from variable assays (GFP or dsRed) were

subjected to the "threshold" followed by "measure" tools in FIJI.[64] To assess PA14::DsRed burden in transgenic animals, regions of interest were generated from the beginning of the intestines (int1) to the posterior end of the worm to prevent the p*myo2*::mCherry co-injection marker signal from interfering with quantifications. When assessing pathogen burden in gravid animals stained with DY96, thresholding was used to quantify spore signal without including signal from embryos.

Pseudomonas aeruginosa infection experiments

For all *Pseudomonas* assays, a single colony was picked into 3 ml of LB and grown overnight at 37°C, 220 rpm for 16-18 hours. 20 µl (for 3.5-cm plate) or 50 µl (for 6-cm plate) of culture was spread onto slow killing (SK) plates to form a full lawn, except in the case of competitive fitness assays (see below). Seeded plates were placed at 37°C for 24 hours, followed by 25°C for 24 hours prior to use. Plates were seeded fresh prior to each experiment. To assess colonization, 1,000 synchronized animals were grown on PA14::dsRED for either 24 or 48 hours at 25°C. Animals were washed off with 1ml M9+ 0.1%Tween-20, and washed twice thereafter, prior to fixation.

To quantify survival of individual strains on PA14, 3.5-cm SK plates were seeded with 20 ul of PA14, to form full lawns. 60 L4s were picked onto each of three, 3.5-cm plates per strain, and 24 hours later, 30 animals from each were picked onto a new 3.5-cm plate (T24hrs). Survival was monitored from 24 hours post L4, three times per day. Survival was assessed based on response to touch. Carcasses were removed, and surviving animals were placed onto fresh 3.5-cm plates every 24 hours. Animals were grown at 25°C for the duration of the experiment. Technical triplicate data was pooled to represent a single biological replicate. The experiment was carried out until no more

worms had survived. Survival curves were generated via GraphPad Prism 9.0, and the Log rank (mantel-cox) test was used to generate P-values.

Transgenic strain construction

N2 or *aaim-1 (kea22)* animals were injected with a 100 ng/µl injection mix composed of 50 ng/µl of template, 5 ng/µl of p*myo2*::mCherry, and 45 ng/µl of pBSK. Three independent lines were generated for each injected construct.

Gateway BP cloning[65,66] was performed to insert AAIM-1 and GFP into pDONR221. Around the horn PCR,[67] was used to insert a 3x Flag sequence at the C-terminus of this construct. Gibson assembly was used to generate different tissue specific clones driving *aaim-1* expression. P*aaim-1, aaim-1* and p*spp-5* were cloned from N2 genomic DNA, *pmyo2* was cloned from pCFJ90. GFP and 3x Flag sequences were cloned from pDD282. *SPΔaaim-1*was amplified from *aaim-1*::3xFlag in pDONR221 by omitting the first 17 amino acids, the putative secretion signal as predicted via SignalP 5.0.[68] All clones possessed an *unc-54* 3' UTR. See Supplemental table 3 for primer sequences.

CRISPR-Cas9 mutagenesis

To generate a deletion allele of *aaim-1* via CRISPR-Cas9 mutagenesis, steps were taken as described here.[69] Briefly, 2 crRNA's were designed using CRISPOR,[70] near the start and stop sites of *aaim-1* and generated via IDT. A repair template was designed to contain 35 base pairs of homology upstream and downstream of the cut sites. *Streptococcus pyogenes* Cas9 3NLS (10ug/ul) IDT and tracrRNA (IDT #1072532) were utilized. Reaction mixes were prepared as

546 described previously.[69] pRF4 was co-injected with the Cas9 ribonucleoprotein, and F1 rollers
547 picked. Deletions were identified via PCR primers situated outside the cut sites.
548
549 **Bead-feeding assays**
550 1,000 synchronized L1 animals were mixed with 0.2 µm green fluorescent polystyrene beads
551 (Degradex Phosphorex) at a ratio of 25:1 in a final volume of 400 µl containing 10 µl of 10x *E.*
552 *coli* OP50, 16 µl of beads and up to 400 µl with M9. Animals were incubated with beads for 3
553 hours, washed off with M9 + 0.1% Tween-20 and fixed with 4% PFA for 30 min at room
554 temperature. Bead accumulation was measured as a percentage of the total animal exhibiting
555 fluorescent signal, using FIJI.
556
557 **Lifespan Assays**
558 Lifespan assays were performed as described previously.[71] In brief, 120 synchronized L4 animals
559 were utilized per strain, with 15 animals placed on a single 3.5-cm NGM plate (A total of 8 plates,
560 with 15 animals each per strain). Animals were transferred to a new seeded 3.5-cm NGM plate
561 every 2 days, for a total of 8 days (4 transfers), ensuring no progeny were transferred alongside
562 adults. After day 8, survival was quantified daily, on the same plate, via response to touch. Any
563 animals that exhibited internal hatching, protruding intestines, or were found desiccated on the
564 edges of the plate were censored. Survival curves were generated via GraphPad Prism 9, and the
565 Log rank (mantel-cox) test was used to generate P values.
566
567 **Immunofluorescence (IF)**

568 IF was performed as described previously,[72] however all steps post-dissection were performed in
569 microcentrifuge tubes, and intestines were pelleted on a mini tabletop microcentrifuge for a few
570 seconds. Briefly, animals were dissected to extrude intestinal tissue. Two 25mm gauge needles on
571 syringes were used to create an incision near the head and/or tail of the animals. Dissections were
572 performed in 5 µl of 10 mM levamisole on glass slides to encourage intestinal protrusion. Fixation,
573 permeabilization and blocking was performed as described previously.[72] Primary M2 anti-Flag
574 antibody (Sigma F1804) was used at 1:250 overnight at 4°C, and secondary goat anti-mouse Alexa
575 fluor 594 (Thermo Fisher A32742) at 1:300 for 1 hour at room temperature. Animals were mounted
576 in 20 µl of EverBrite™ Mounting Medium (Biotium) and placed on glass slides for imaging.
577
578 **Competitive fitness assays**
579 N2 or *aaim-1* mutants were grown together with RFP::Znfx1 YY1446 *(gg634)*, which labels the
580 germ granules and can be observed in all developmental stages[73]. For *N. parisii* infections, 10-cm
581 NGM plates were seeded with 1 ml of 10xOP50 and a medium-2 dose of spores (no spores were
582 used for uninfected plates). 10 L1s from each strain were picked onto lawns of spores and *E. coli*
583 OP50 immediately after drying, and grown for 8 days at 21°C, washed off with M9 + 0.1% Tween-
584 20, and fixed. For *P. aeruginosa* infections, 3.5-cm SK plates were seeded with a single spot of 20
585 µl of PA14 in the center of the plate. 10 L1s of each strain were placed on plates and grown at
586 21°C for 8 days and then washed off with M9 + 0.1% Tween-20. The percentage of animals that
587 did not display RFP germ granules (i.e. N2 or *aaim-1* mutants) is was determined by quantifying
588 all animals on the plate, including F1 adults and L1/L2 staged F2 animals.
589
590 **Co- infections with *N. parisii* and *P. aeruginosa***

Co-infection assays were performed by first pulse infecting co-infection and *N. parisii* single infection groups with an maximal dose of spores for three hours on unseeded 6-cm NGM plates as described above. PA14::DsRed single infections were pulsed with a volume of M9 to match that of the spores. Animals were then washed off in 1ml of M9 + 0.1%Tween-20, followed by 2 more washes, prior to placement on full lawns of PA14::DsRed on a 6-cm SK plates prepared as described above. *N. parisii* single infections were placed on a 6-cm NGM plate pre-seeded with 200 µl of 10xOP50. Plates were incubated at 21°C.

Phylogenetic analysis

Homology between AAIM-1 and other proteins was determined with protein BLAST (https://blast.ncbi.nlm.nih.gov/Blast.cgi) using default parameters. Sequences with less than E-5 were aligned using MUSCLE (https://www.ebi.ac.uk/Tools/msa/muscle/) using default parameters. Phylogenetic tree of homologs was generated using RAxML BlackBox https://raxml-ng.vital-it.ch/#/ using default parameters and 100 boot straps. Tree was visualized using FigTree v1.4.4 (http://tree.bio.ed.ac.uk/software/figtree/).

Statistical analysis

All data analysis was performed using GraphPad Prism 9.0. One-way Anova with post hoc (Tukey test) was used for all experiments unless otherwise specified in figure legends. Statistical significance was defined as $p < 0.05$.

Acknowledgements

We thank Ashley M. Campbell, Alexandra R. Willis, and Kristina Sztanko for providing helpful comments on the manuscript. This work was supported by the Canadian Institutes of Health Research grant no. 400784 and an Alfred P. Sloan Research Fellowship FG2019-12040 (to A.W.R.). This work was supported by National Institutes of Health (www.nih.gov) under R01 AG052622 and GM114139 to E.R.T. Some strains were provided by the CGC, which is funded by NIH Office of Research Infrastructure Programs (P40 OD010440) and we thank WormBase.

Author contributions:

H.T.E.J. and A.W.R. designed experiments, analyzed results, and co-wrote the paper.

H.T.E.J. conducted all experiments, except the initial forward genetic screen performed by **A.W.R.**

C.M. designed and performed bioinformatic analysis for the MIP-map experiment.

M.R.S. analyzed whole genome sequencing to identify causal mutations in *fawn* animals.

E.R.T., A.G.F., and A.W.R. provided mentorship and acquisition of funding.

Competing interests: The authors declare they have no competing interests.

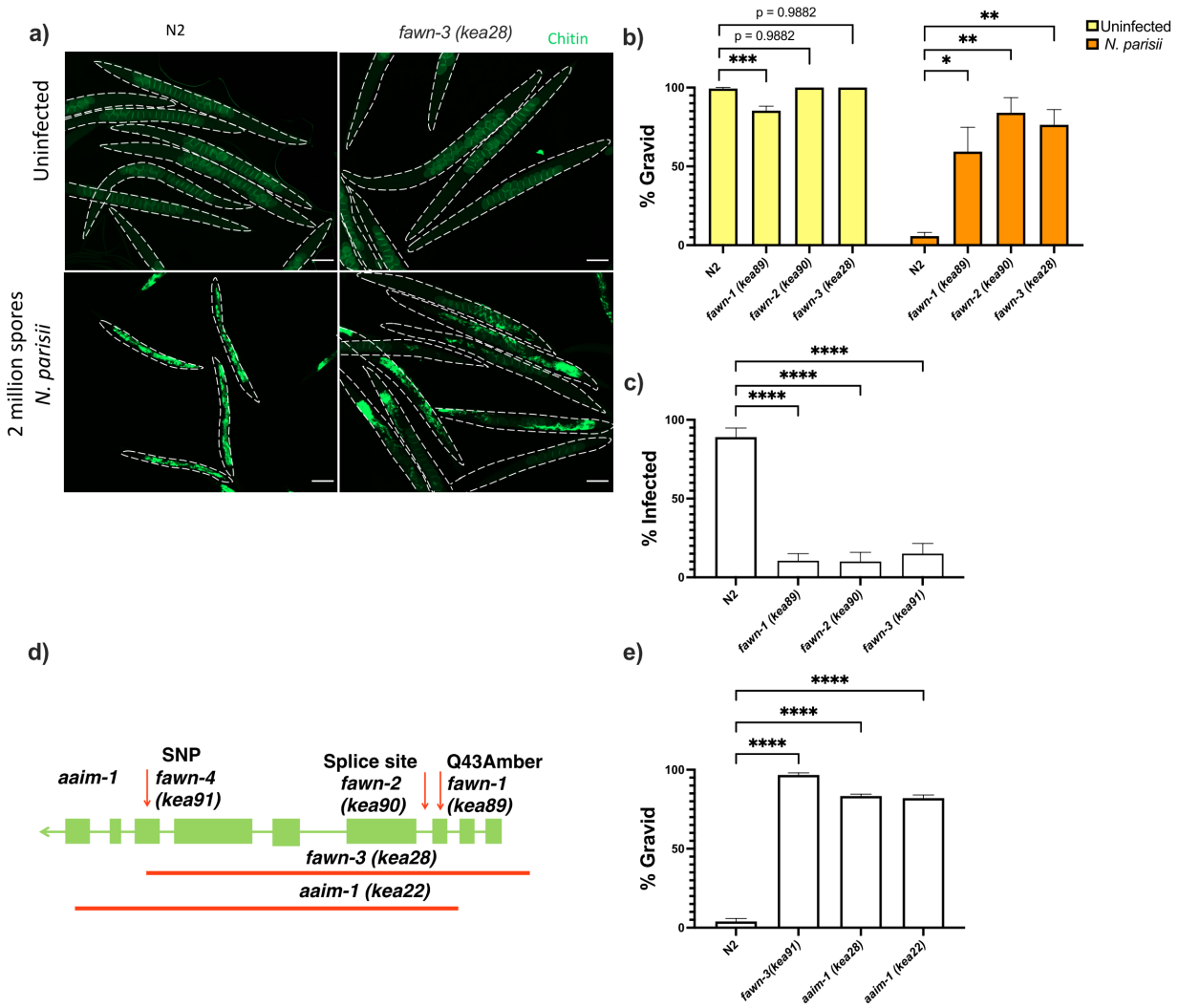

629

630 **Figure 1: Mutations in *aaim-1* result in resistance to *N. parisii* infection.**

631 (a-c, and e) L1 stage Wild-type (N2) and *aaim-1* mutant animals were infected with either a high
632 dose (a, b, and e) or a very lose dose (c) of *N. parisii*, fixed at 72 hours, and stained with direct-
633 yellow 96 (DY96). (a) Representative images stained with DY96, which stains *C. elegans* embryos
634 and microsporidia spores. Scale bars, 100 μm. (b and e) Percentage of worms that are gravid. (c)
635 Percentage of worms that contain newly formed *N. parisii* spores. (d) Schematic depicting the
636 nature and location of the different *aaim-1* alleles. Boxes represent exons, and connecting lines
637 represent introns. Arrows depict point mutations, and the solid red line depicts deletions. *fawn-3*

638 has a 2.2 kb deletion and *aaim-1 (kea22)* has a 2.3 kb deletion. *fawn-1* carries a C127T , Q43Stop
639 mutation, *fawn-2* carries a G221A splice site mutation and *fawn-4* carries a C1286T, A429V
640 mutation in *aaim-1*.(b,c, and e) Data is from three independent replicates with at least 90 animals
641 counted per replicate. Mean ± SEM represented by horizontal bars. P-values determined via one-
642 way ANOVA with post hoc. Significance defined as: * $p < 0.05$, ** $p < 0.01$, *** $p < 0.001$, ****
643 $p < 0.0001$.

644

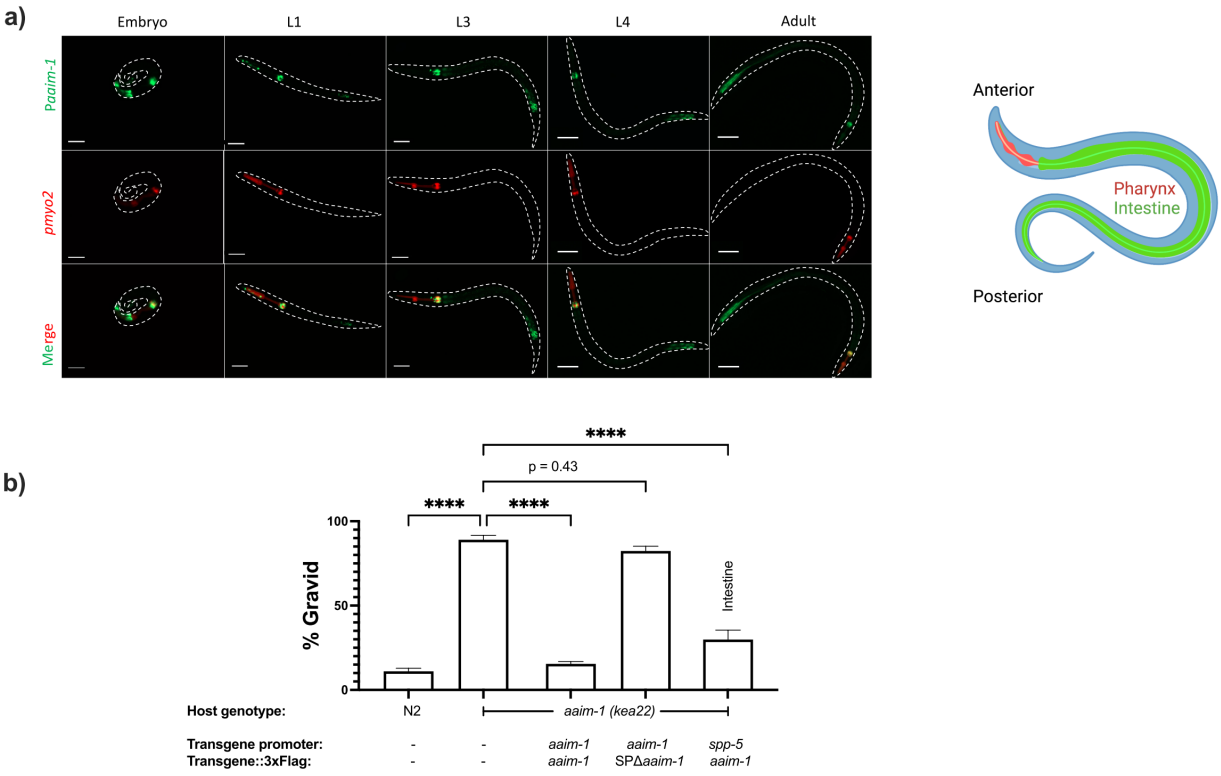

645

646

647

Figure 2: AAIM-1 is secreted from intestinal cells.

(a) Wild-type worms containing an extrachromosomal array expressing GFP from the *aaim-1* promoter and mCherry in the pharyngeal muscles were imaged at the embryo, L1, L3, L4, and adult stage. Embryo, L1 and L3 animals were imaged at 40x, scale bar 20 μm and L4 and adult animals were imaged at 20x, scale bar 50 μm. L1 to L4 are oriented anterior to posterior and adult oriented posterior to anterior from left to right. Schematic made with Biorender.com (b) N2, *aaim-1, and aaim-1* expressing extrachromosomal arrays were infected with a medium-2 dose of *N. parisii*. Percentage of worms that are gravid. Experiment is from three independent replicates with at least 90 worms quantified per replicate. Mean ± SEM represented by horizontal bars. P-values determined via one-way ANOVA with post hoc. Significance defined as **** $p < 0.0001$ (c) Intestines (denoted by dashed lines) of 72-hour post-L1 adults were dissected and stained using anti-Flag (red) and DAPI (blue). Images taken at 40x, scale bar 20 μm.

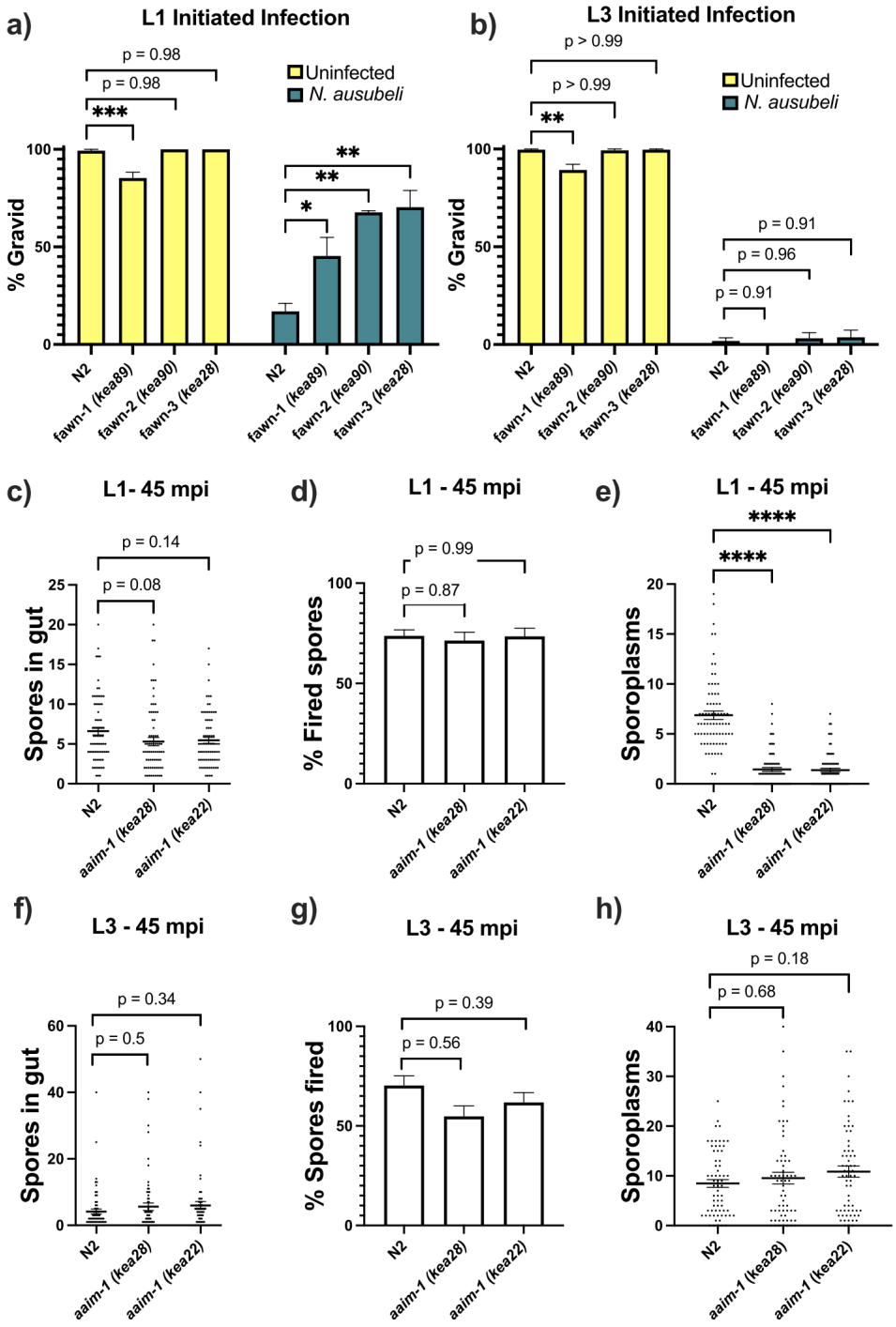

Figure 3: *aaim-1* mutants are resistant to microsporidia at the earliest larval stage due to spore misfiring. (a-b) N2 and *aaim-1* mutants were infected with a medium dose of *N. ausubeli* at either the L1 stage for 72 hours (a) or a high doses of *N. ausubeli* at the L3 stage for 48 hours

(b) Percentage of worms that are gravid. (c-f) N2 and *aaim-1* animals were infected with a medium-3 dose of *N. parisii* for 45 minutes at L1 (c-e) or L3 hours (f-h), fixed, and then stained with DY96 and *N. parisii* 18S RNA fish probe. The number of spores per animal (c,f), the percentage of spores fired (d,g), and the number of sporoplasm per worm (e,h) are displayed. (a-b) Experiment is of three replicates of at least 100 animals. (c-h) Experiment is of three replicates of 20-30 animals. (a-h) Mean ± SEM represented by horizontal bars. P-values determined via one-way ANOVA with post hoc. Significance defined as: * $p < 0.05$, ** $p < 0.01$, *** $p < 0.001$, **** $p < 0.0001$.

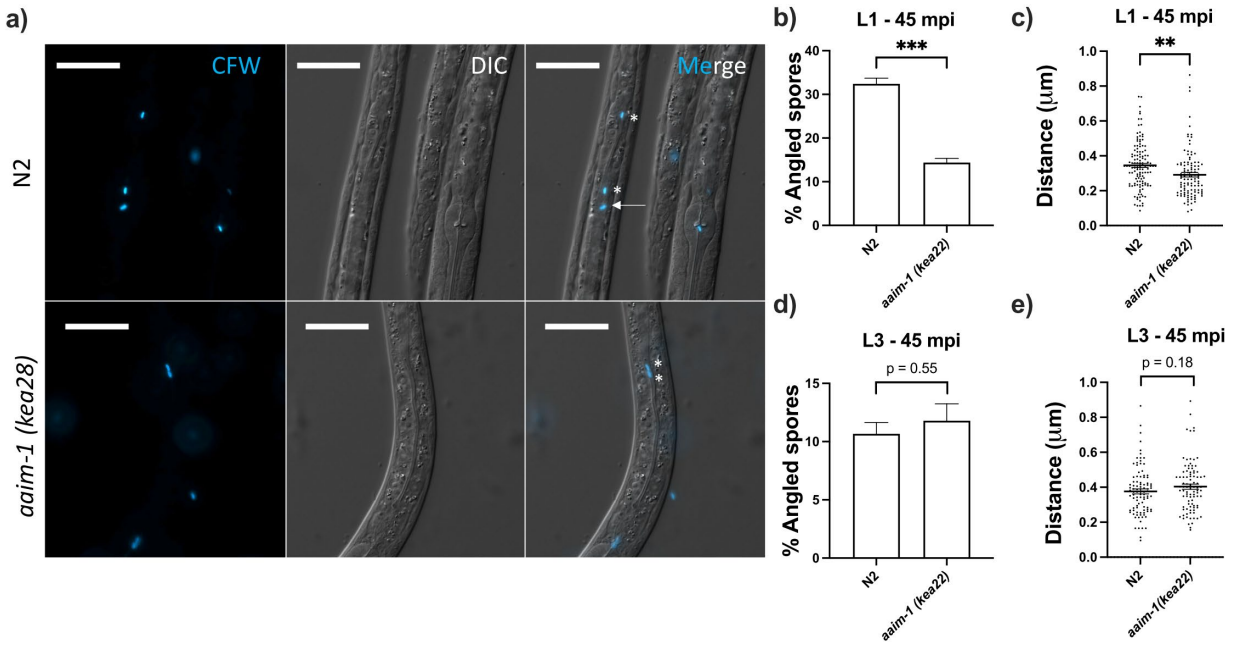

Figure 4: Spores in *aaim-1* mutants display improper orientation and distance to the apical intestinal membrane.

(a-e) N2 and *aaim-1(kea22)* animals were infected with a very high dose of Calcofluor white (CFW) pre-stained *N. parisii* spores for 45 minutes at either the L1 stage (a-c) or the L3 stage (d-e). (a) Representative images of live animals containing stained spores (blue). Arrow indicates an example of an angled spore, asterisks indicate parallel spores. Images taken at 40x, scale bar 20 µm. (b, d) Percentage of angled spores. The experiment consists of three replicates with at least 90 spores per replicate. (c, e) Distance of the center of each spore from the intestinal apical membrane. The experiment consisted of three replicates of at least 25 spores per replicate. Mean ± SEM represented by horizontal bars. P-values determined via unpaired Student's t-test. Significance defined as ** $p < 0.01$, *** $p < 0.001$.

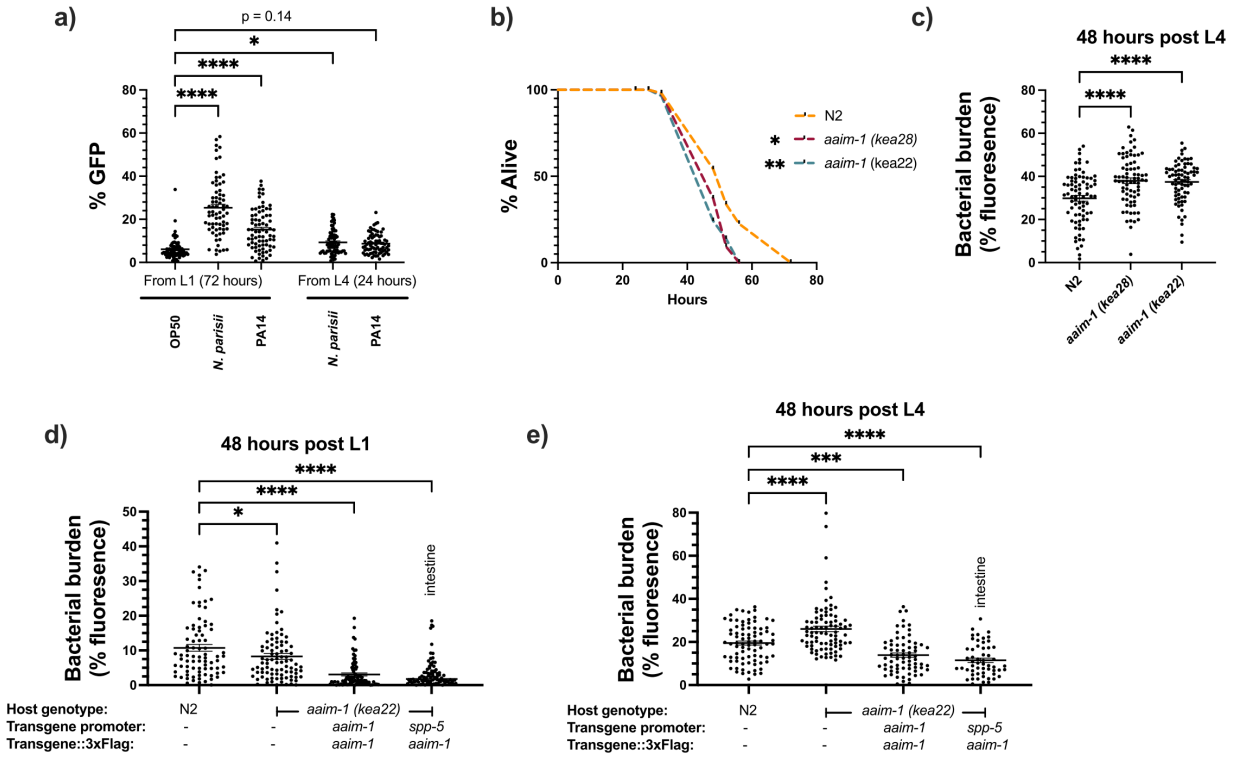

Figure 5: *aaim-1* is upregulated by *N. parisii and P. auerginosa* and *aaim-1* animals are susceptible to infection by *P. aeruginosa*.

(a) Expression of p*aaim-1*GFP::3xFlag in response to infection with either PA14 or *N. parisii* for either 72 hours from L1 or 24 hours from L4. 18-25 animals quantified per replicate. Every point represents a single worm. Percentage GFP was measured as the percentage of the animal containing GFP via FIJI. n=3. (b) L4 stage N2 and *aaim-1* were plated on full lawns of *P. aeruginosa* PA14 and the percentage of animals alive was counted over the course of 96 hours. Three independent replicates were carried out, and a representative replicate is displayed. 40 worms were quantified per strain. P-values determined via Log-rank (Mantel-Cox) test. Significance defined as * $p < 0.05$, ** $p < 0.01$. (c-e) N2, *aaim-1,* or *aaim-1* with different extrachromosomal arrays were plated on PA14::DsRed as either L1 stage (d) or L4 stage (c,e) for 48 hours. Bacterial burden was measured as the percentage of the animal containing

PA14::dsRED. Three independent replicates carried out, 20-30 worms were quantified per replicate. Every point represents a single worm. Mean ± SEM represented by horizontal bars. (a, c-e) P- values determined via one-way ANOVA with post hoc. Significance defined as * $p < 0.05$, ** $p < 0.01$, *** $p < 0.001$, **** $p < 0.0001$.

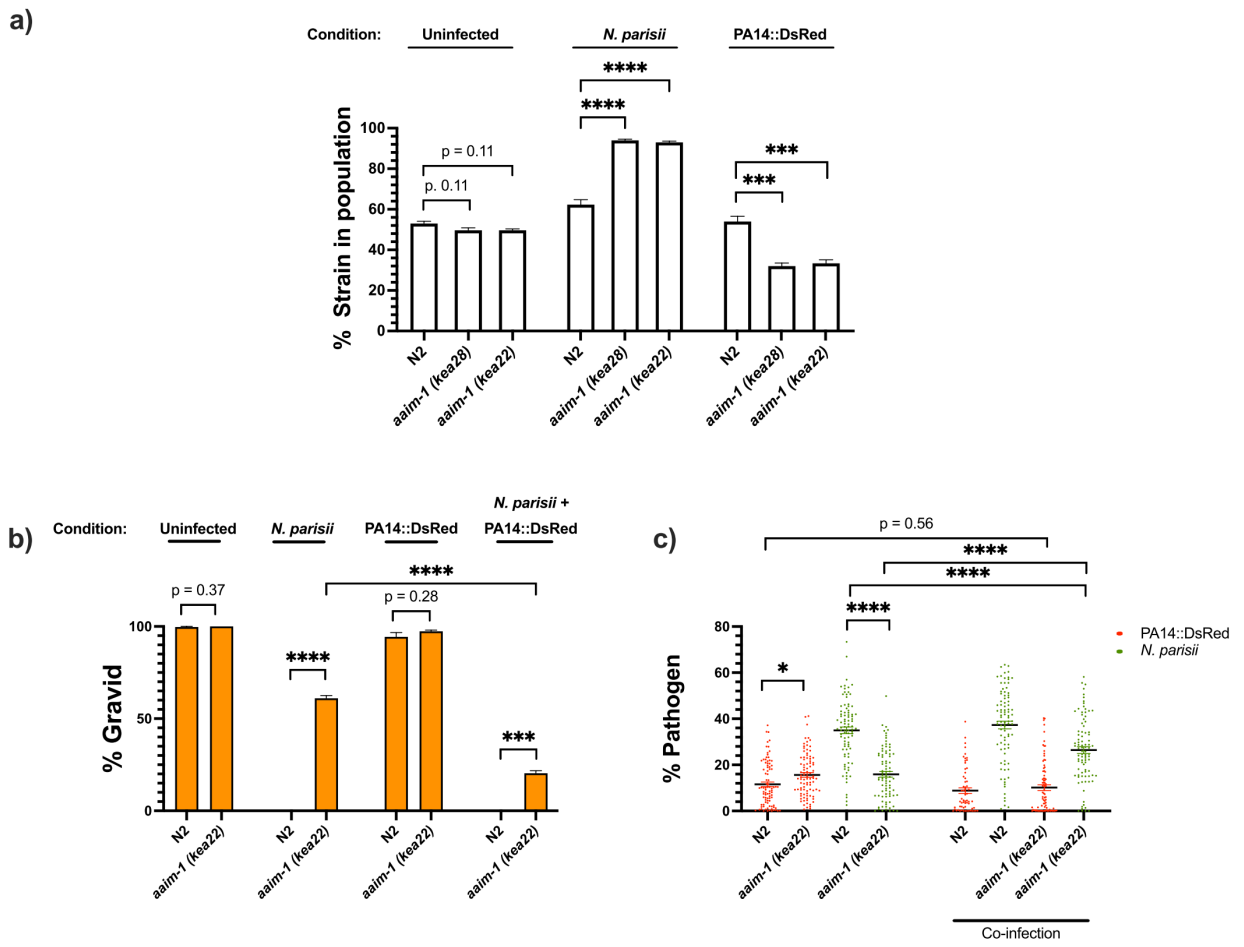

715

716 **Figure 6: *aaim-1* alleles display enhanced fitness on *N. parisii*, but reduced fitness on *P.***
717 ***aeruginosa*.**

718 (a) Competitive fitness assays performed with a fluorescently marked strain (RFP::ZNFX1) mixed
719 with either N2 or *aaim-1* mutants. These mixed populations of animals were plated at the L1 stage
720 on either *E. coli*, a medium-2 dose of *N. parisii*, or on *P. aeruginosa*. After 8 days, the fraction of
721 animals that did not display fluorescent germ granules was counted. Experiment consisted of three
722 replicates with 20-270 worms quantified per replicate. (b,c) L1 N2 and *aaim-1* animals were either
723 uninfected or infected with a maximal dose of *N. parisii*. These infected and uninfected population
724 of animals were then washed and placed on either *E. coli* or PA14::DsRed. After 69 hours, animals
725 were fixed and stained with DY96. Experiment consisted of three replicates with 60-150 worms

726 quantified per replicate. (b) Percentage of animals that are gravid adults. (c) Quantified amount of
727 either *N. parisii* (DY96) or *P. aeruginosa* (PA14::DsRed). 12-30 worms were quantified per
728 replicate. Mean ± SEM represented by horizontal bars. P-values determined via unpaired Student's
729 t-test (a) one-way ANOVA with post hoc (b,c). Significance defined as ** $p < 0.01$, *** $p < 0.001$,
730 **** $p < 0.00$

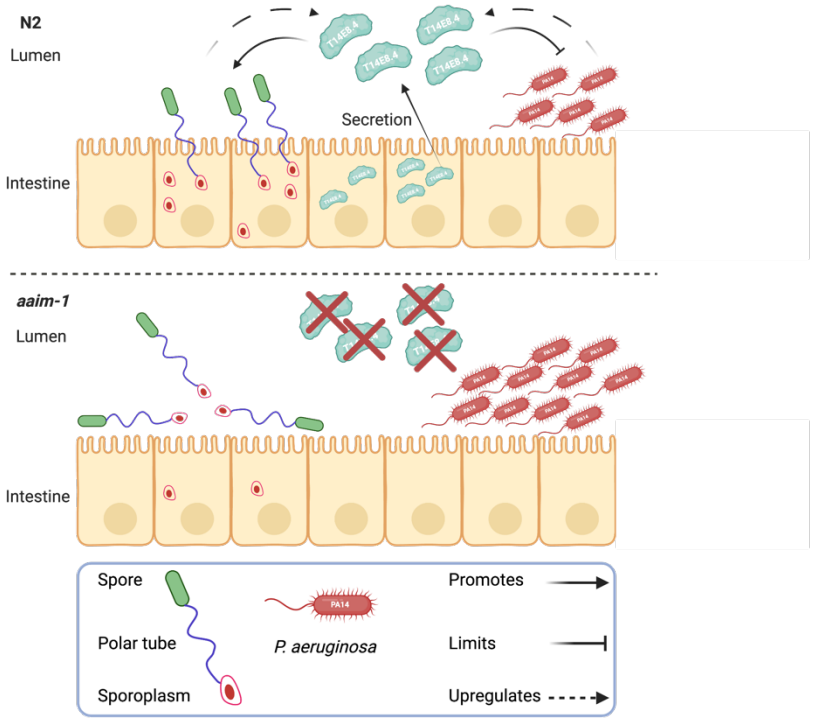

731

732 **Figure 7: Secreted AAIM-1 functions in the intestinal lumen to limit bacterial colonization**
733 **but is exploited by microsporidia to ensure successful invasion of intestinal cells**.
734 AAIM-1 is secreted from intestinal cells, where the protein limits bacterial colonization in the
735 lumen. Additionally, AAIM-1 is parasitized by *N. parisii* spores to ensuring successful orientation
736 and firing during intestinal cell invasion. Infection by either of these two pathogens results in the
737 upregulation of AAIM-1. Figure made with Biorender.com.

Supplemental material

Figure S1. Mapping and validation of *aaim-1* as the gene associated with resistance to *N. parisii*.

Figure S2: AAIM-1 is conserved in both free-living and parasitic nematodes.

Figure S3: *aaim-1* is expressed in arcade cells and presence of C-terminal 3x Flag tag does not disrupt AAIM-1 function.

Figure S4: *aaim-1* mutants do not clear *N. parisii* and developmentally restricted *N. parisii* invasion defect is not due to a feeding defect.

Figure S5: Invasion defects in *aaim-1* only occurs at the L1 stage of development and a mutation in *aaim-1* do not alter the width of the intestinal lumen.

Figure S6: Susceptibility to *P. aeruginosa* PA14 appears at L4.

Figure S7: A mutation in *aaim-1* does not influence *C. elegans* lifespan.

Figure S8: List of naturally occurring *aaim-1* variants in wild isolates of *C. elegans*.

Supplemental table 1: List of strains utilized in this study

Supplemental table 2: Spore doses utilized in this study.

Supplemental table 3: Primer sequences.

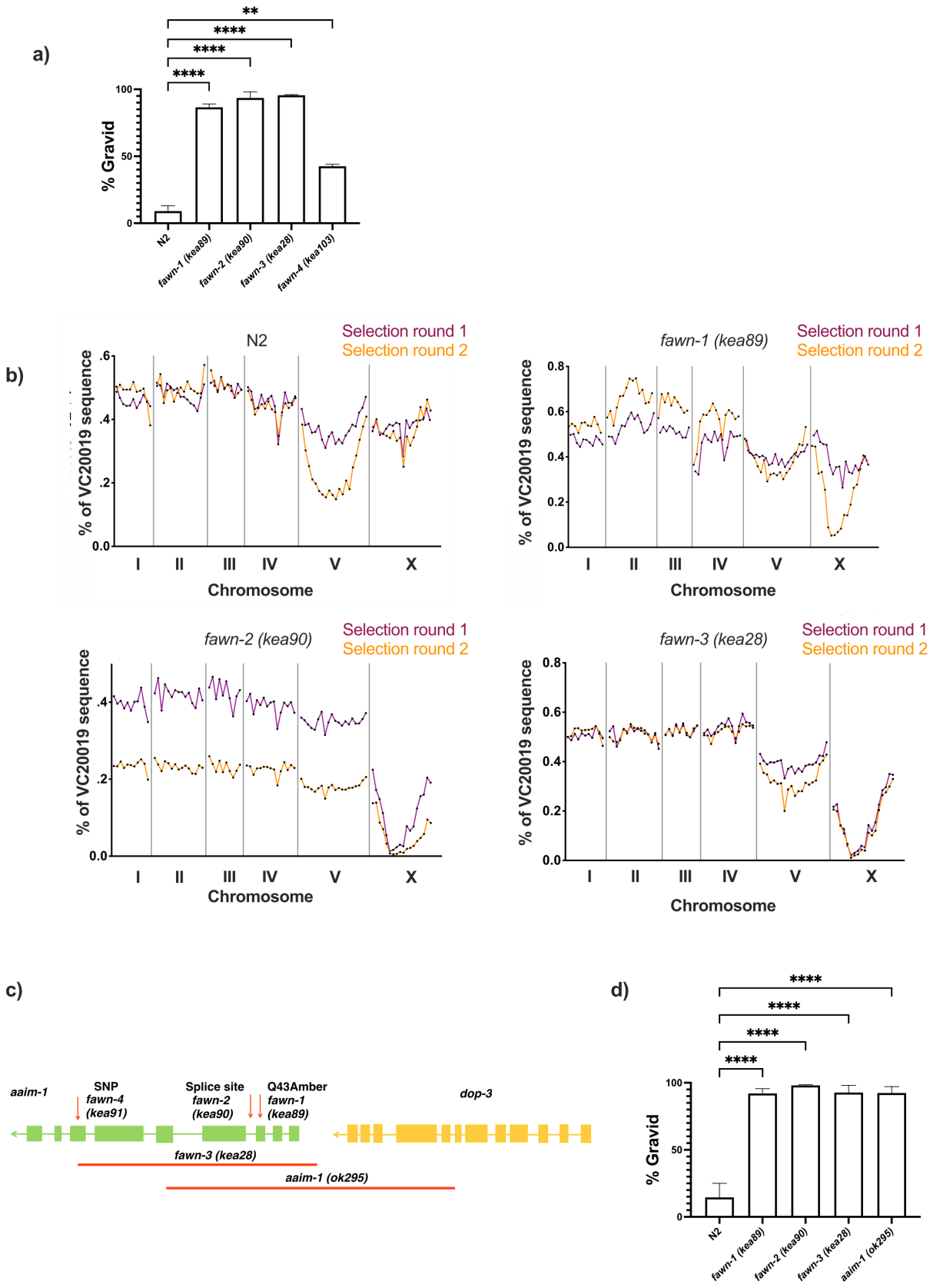

758

Figure S1. Mapping and validation of *aaim-1* as the gene associated with resistance to *N. parisii*.

(a) N2 or *fawn* animals were infected with a medium-3 dose of *N. parisii* spores on 6-cm plates, fixed at 72 hours, and stained with direct-yellow 96 (DY96). Graph displays percentage of worms that are gravid. Experiment consists of two independent replicates with 66-300 worms quantified per replicate. (b) F2 recombinants between the mapping strain VC20019 and either N2, *fawn-1*, *fawn-2*, or *fawn-3* were infected with a medium-2 dose of *N. parisii*. Two rounds of selection were performed (see methods). The percentage of sequencing reads mapping to the reference strain VC20019 are depicted on the Y axis, and the linkage groups are depicted on the X axis. Sequencing of MIPs resulted in capturing the identity of the genome at 89 distinct regions which are represented as points by their location along the X-axis coordinates. A significantly diminished percentage of VC20019 indicates an enrichment of non-mapping genomic sequence in that region. (c) Schematic representing the location and nature of the different *aaim-1* alleles. Boxes represent exons, and connecting lines represent introns. Arrows represent point mutations and solid red lines represent large deletions. *fawn-3* has a 2.2 kb deletion and *aaim-1 (kea22)* has a 2.3 kb deletion. RB563 *(ok295)* possesses a large deletion overlapping two different genes, *aaim-1* and *dop-3*, the boundaries of which are unclear.[40,74] (d) L1 stage N2 and *aaim-1* mutant animals were infected with a high dose of *N. parisii*, fixed at 72 hours, and stained with direct-yellow 96 (DY96). Percentage of gravid worms is shown. Experiment consists of three independent replicates with at least 100 worms quantified per replicate. Mean ± SEM represented by horizontal bars. P-values determined via One-way Anova with post hoc. Significance defined as **** $p < 0.0001$.

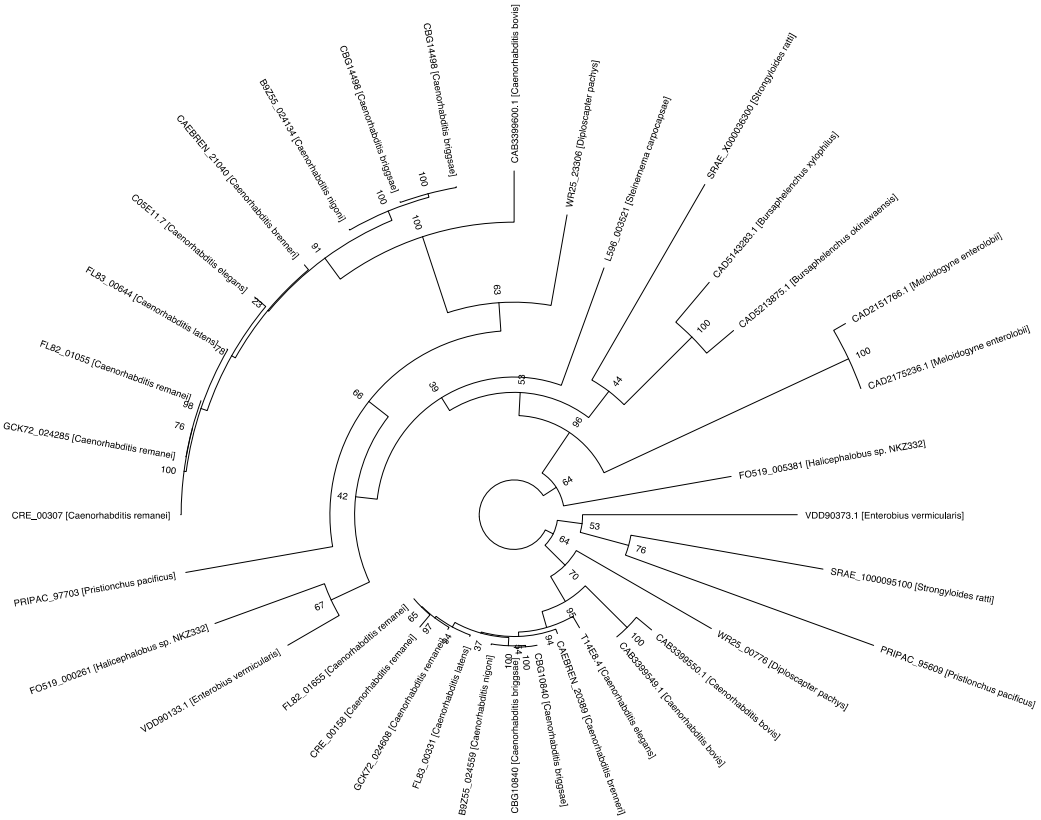

Figure S2: Homologs of AAIM-1 are present in both free-living and parasitic nematodes. Phylogenetic tree of AAIM-1 homologs. Bootstrap values are shown at the nodes.

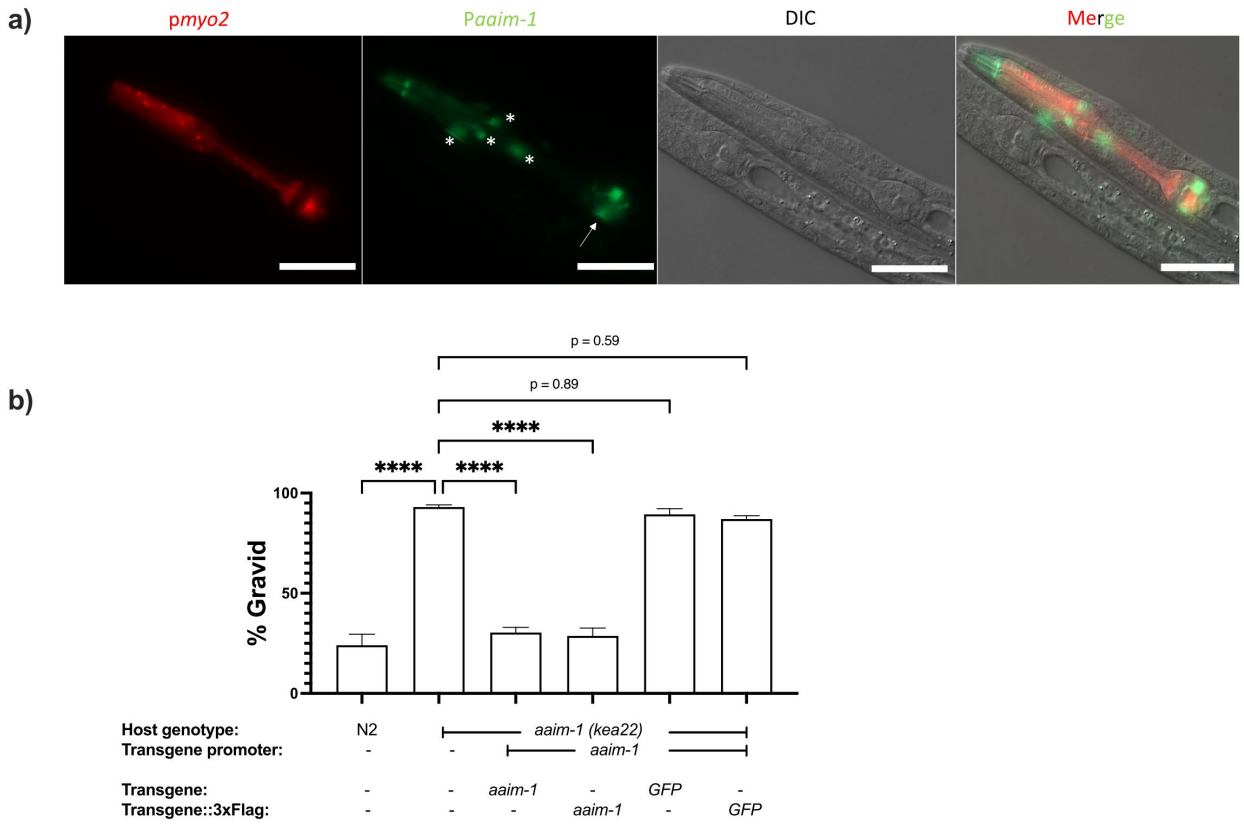

791

792 **Figure S3: *aaim-1* is expressed in arcade cells and presence of C-terminal 3x Flag tag does**

793 **not disrupt AAIM-1 function.**

794 (a) N2 containing an extrachromosomal array expressing GFP from the *aaim-1* promoter and

795 mCherry in the pharyngeal muscles were imaged at the L1 stage at 40x. Scale bar 20 μm. Arrow

796 indicates terminal bulb, and asterisks represent arcade cells. (b) N2, *aaim-1,* and *aaim-1* expressing

797 extrachromosomal arrays of wild-type or 3x Flag tagged constructs were infected with a medium-

798 2 dose of *N. parisii*, fixed at 72 hours, and stained with direct-yellow 96 (DY96). Percentage of

799 gravid worms is shown. Experiment is of three independent replicates of at least 100 animals each.

800 Mean ± SEM represented by horizontal bars. P-values determined via one-way ANOVA with post

801 hoc. Significance defined as **** $p < 0.0001$.

802

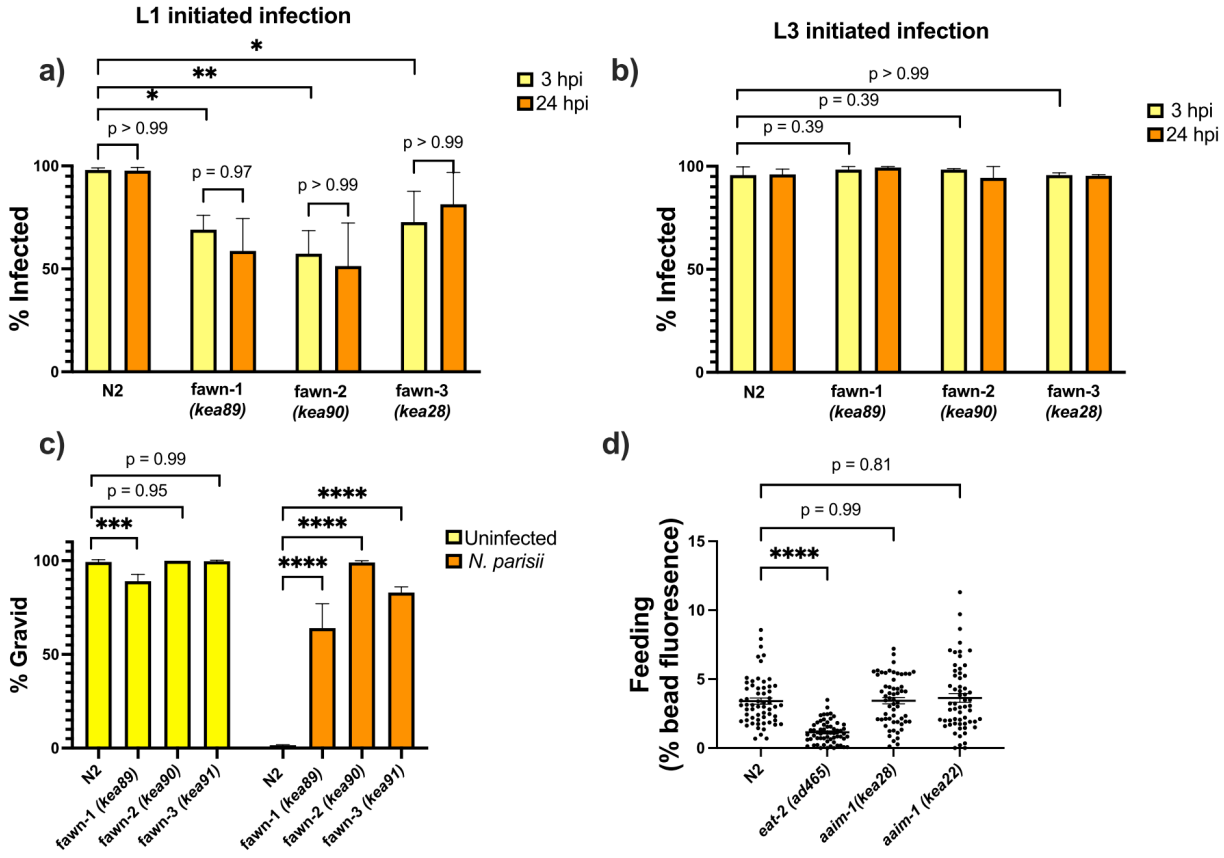

Figure S4: *aaim-1* mutants do not clear *N. parisii* and developmentally restricted *N. parisii* invasion defect is not due to a feeding defect. (a-b) N2 and *aaim-1* mutants were infected at either the L1 stage (a) or the L3 stage (b) with a medium-1 dose of *N. parisii* spores for 3 hours. Animals were then washed to remove spores and re-plated for an additional 21 hours. Worms were fixed at both the 3 hour and 24 hour timepoints and stained with an *N. parisii* 18S RNA fish probe. Worms containing either sporoplasm or meronts were counted as infected. (c) N2 and *aaim-1* adults were allowed to lay embryos on plates. Adults were removed and a low dose of *N. parisii* was added to the plate. Animals were fixed at 72 hours and stained with direct-yellow 96 (DY96). Percentage of gravid worms is shown. (d) N2 and *aaim-1* mutants were fed fluorescent beads for 3 hours. Quantitation of percentage of worm with bead fluorescence. Three replicates were performed experiment with at least 100 worms (a-c) or 20-30 worms (d) quantified per replicate.

Mean ± SEM represented by horizontal bars. P-values determined via one-way ANOVA with post hoc. Significance defined as * $p < 0.05$, ** $p < 0.01$, *** $p < 0.001$, **** $p < 0.0001$.

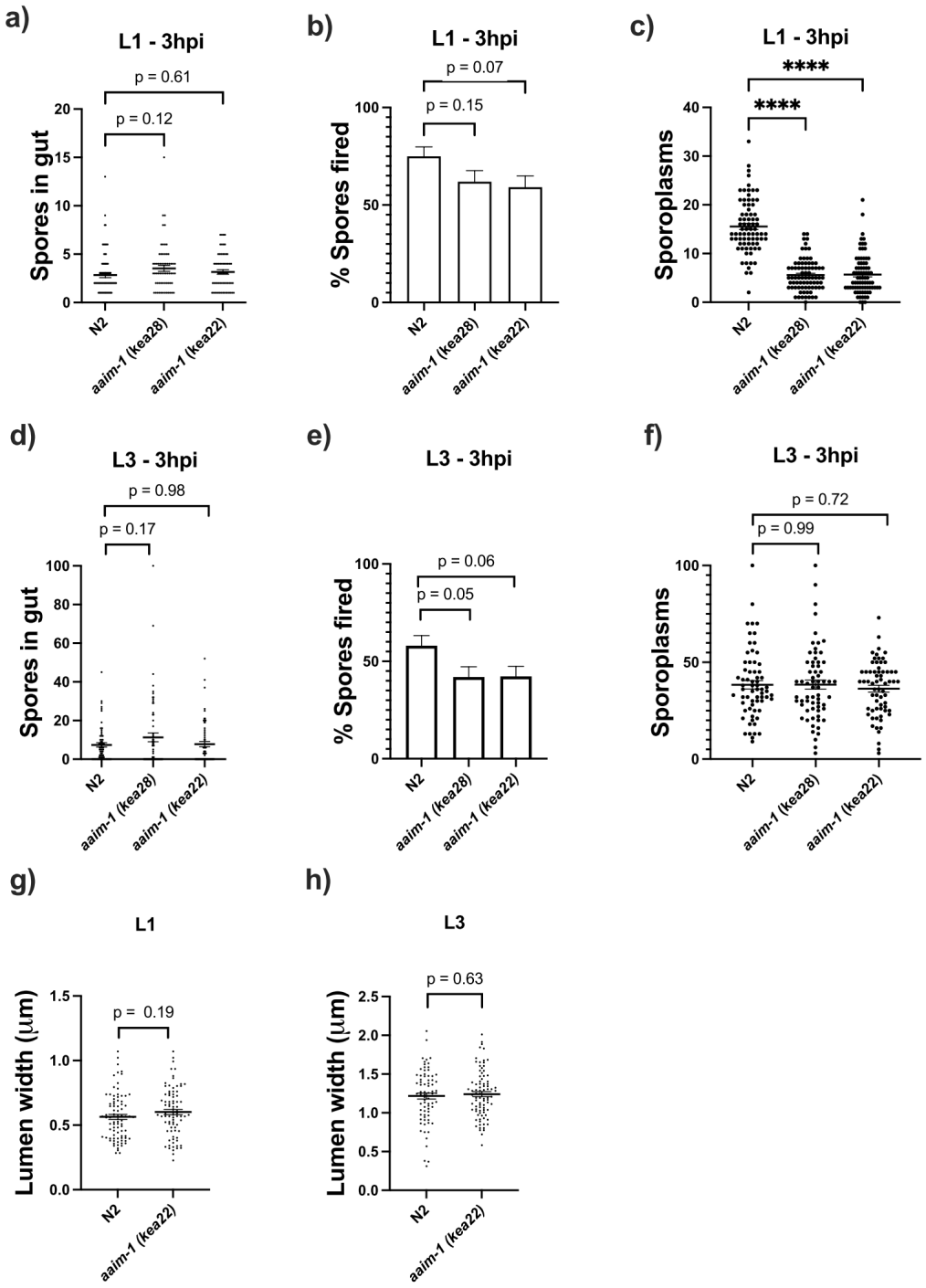

826

827 **Figure S5: Invasion defects in *aaim-1* only occurs at the L1 stage of development and a**

828 **mutation in *aaim-1* do not alter the width of the intestinal lumen.**

829 (a-f) N2 and *aaim-1* animals were infected for 3 hours at L1 (a-c) or L3 (d-f), fixed, and then
830 stained with DY96 and an *N. parisii* 18S RNA fish probe. The number of spores per animal (a,d)
831 the percentage of spores fired (b,e) and the number of sporoplasm per worm (c,f) are displayed.
832 (g,h) The width of the intestinal lumen was measured in L1 (g) or L3 (h) wild-type or *aaim-1*
833 animals. (a-h) Experiment is of 3 replicates of 16-30 animals each. Mean ± SEM represented by
834 horizontal bars. P-values determined via one-way ANOVA with post hoc (a-f) or Unpaired
835 Student's t-test (g,h). Significance defined as **** $p < 0.0001$.
836
837
838
839
840
841

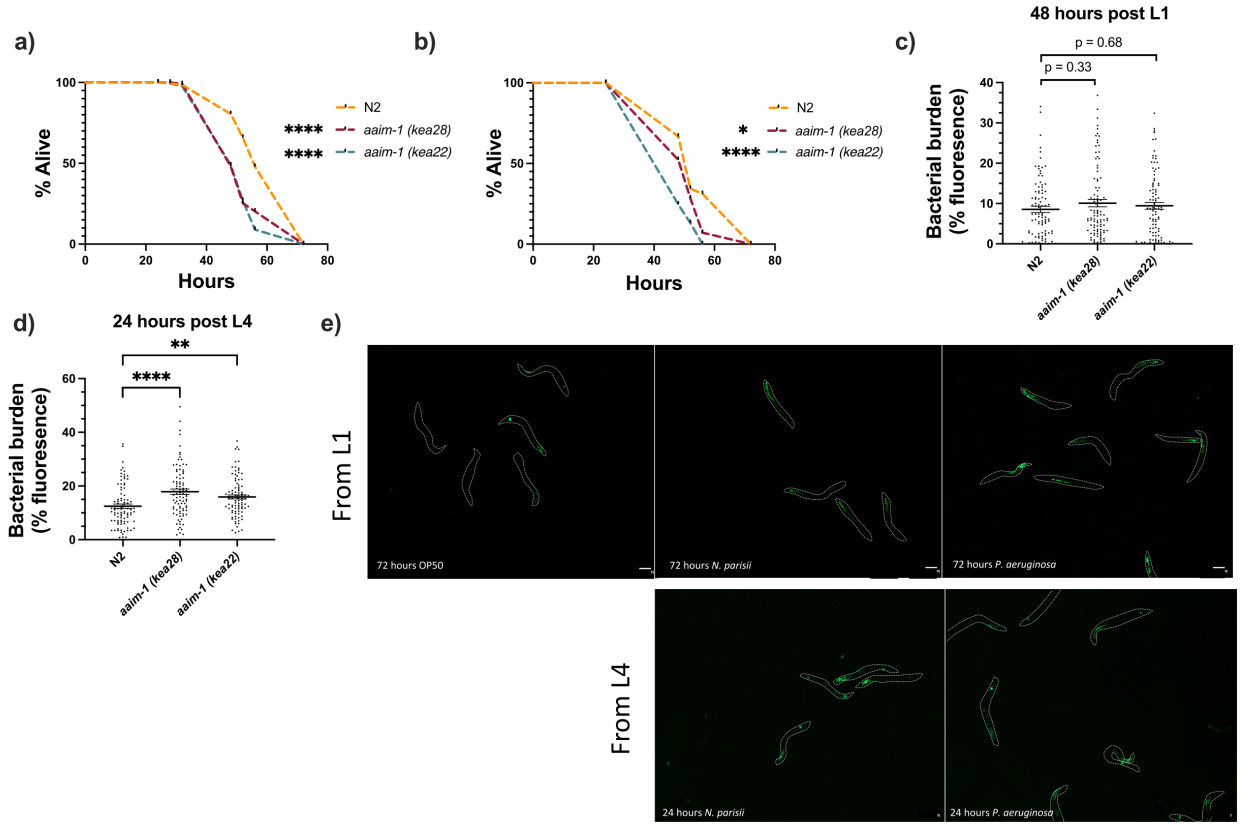

842

843 **Figure S6: Susceptibility to *P. aeruginosa* PA14 appears at L4.**

844 (a,b) Additional replicates of survival assays of animals grown on full lawns of PA14 as in Figure
845 5a. (c-d) N2 and *aaim-1* mutants were grown on PA14::DsRed 48 hours post L1 (c) or 24 hours
846 post L4 (d). Experiment is of three replicates, with 20-30 worms were quantified per replicate via
847 FIJI. Every point represents a single worm. Bacterial burden was measured as the percentage of
848 the animal containing PA14::dsRED via FIJI. Mean ± SEM represented by horizontal bars. (e)
849 p*aaim-1*::GFP::3xFlag were exposed to either PA14 or *N. parisii* 72 hours post L1 or 24 hours
850 post L4. Animals were Imaged at 45.5x, scale bar 500 μm. P-values determined via one-way
851 ANOVA with post hoc. Significance defined as ** $p < 0.01$, **** $p < 0.0001$.

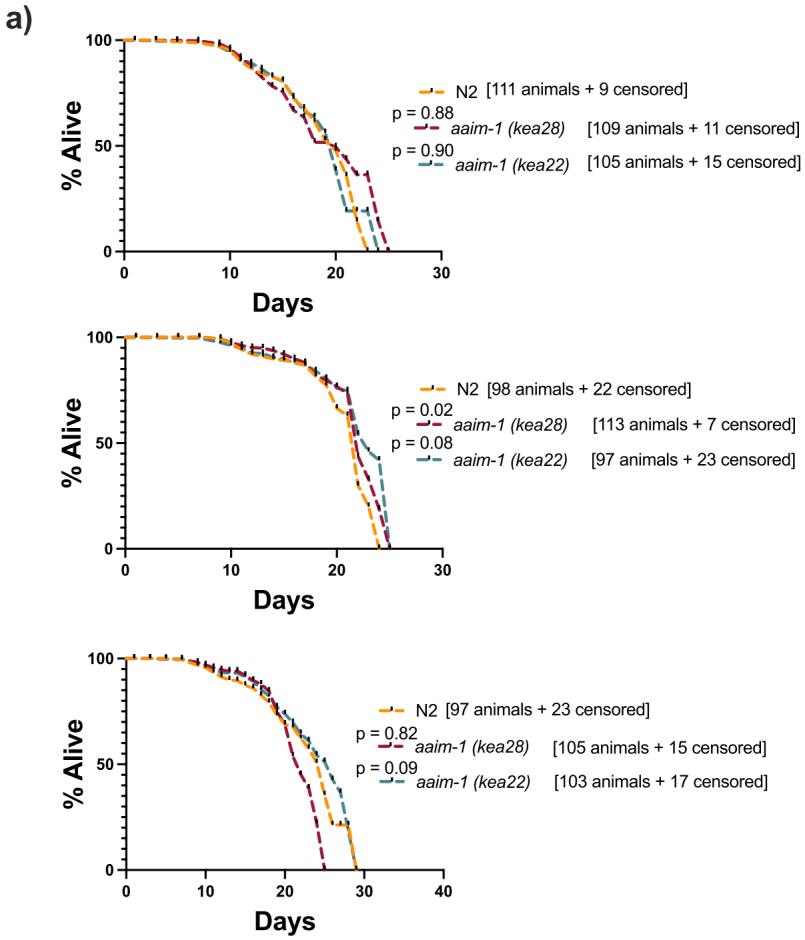

852

853 **Figure S7: A mutation in *aaim-1* does not influence *C. elegans* lifespan.**

854 N2 and *aaim-1* mutants were grown on *E. coli* OP50 for one month, and survival measured as
855 number of animals responsive to touch. The number of animals quantified, as well as those
856 censored are denoted on the graph. Three independent survival assays are displayed. P-values
857 determined via Log-rank (Mantel-Cox) test.

T14E8.4 (X-6559570-6562366)

CHROM	POS	REF	ALT	AF	allele	effect	impact	gene_name	gene_id	feature_id	transcript_biotype	nt_change	aa_change
X	6559573	A	G	0	G	synonymous_variant	LOW	T14E8.4	WBGene00043981	T14E8.4.1	protein_coding	c.1545T>C	p.Asn515Asn
X	6560363	A	G	0	G	synonymous_variant	LOW	T14E8.4	WBGene00043981	T14E8.4.1	protein_coding	c.1284T>C	p.Ser428Ser
X	6560426	A	G	0	G	synonymous_variant	LOW	T14E8.4	WBGene00043981	T14E8.4.1	protein_coding	c.1221T>C	p.Tyr407Tyr
X	6560445	T	TA	0	TA	splice_region_variant&intron_variant	LOW	T14E8.4	WBGene00043981	T14E8.4.1	protein_coding	c.1204-3_1204-2insT	NA
X	6560485	A	G	0.77	G	splice_region_variant&intron_variant	LOW	T14E8.4	WBGene00043981	T14E8.4.1	protein_coding	c.1203+7T>C	NA
X	6560524	C	G	0	G	missense_variant	MODERATE	T14E8.4	WBGene00043981	T14E8.4.1	protein_coding	c.1171G>C	p.Val391Leu
X	6560647	C	A	0.02	A	missense_variant	MODERATE	T14E8.4	WBGene00043981	T14E8.4.1	protein_coding	c.1048G>T	p.Ala350Ser
X	6560670	A	G	0	G	missense_variant&splice_region_variant	MODERATE	T14E8.4	WBGene00043981	T14E8.4.1	protein_coding	c.1025T>C	p.Val342Ala
X	6560810	T	A	0.01	A	missense_variant	MODERATE	T14E8.4	WBGene00043981	T14E8.4.1	protein_coding	c.940A>T	p.Ile314Phe
X	6560841	G	A	0.01	A	synonymous_variant	LOW	T14E8.4	WBGene00043981	T14E8.4.1	protein_coding	c.909C>T	p.Thr303Thr
X	6560869	A	T	0.02	T	missense_variant	MODERATE	T14E8.4	WBGene00043981	T14E8.4.1	protein_coding	c.881T>A	p.Val294Glu
X	6560873	C	T	0.01	T	missense_variant	MODERATE	T14E8.4	WBGene00043981	T14E8.4.1	protein_coding	c.877G>A	p.Val293Ile
X	6560876	T	C	0	C	missense_variant	MODERATE	T14E8.4	WBGene00043981	T14E8.4.1	protein_coding	c.874A>G	p.Lys292Glu
X	6560955	C	T	0	T	synonymous_variant	LOW	T14E8.4	WBGene00043981	T14E8.4.1	protein_coding	c.795G>A	p.Ser265Ser
X	6561004	C	T	0.09	T	missense_variant	MODERATE	T14E8.4	WBGene00043981	T14E8.4.1	protein_coding	c.746G>A	p.Arg249Lys
X	6561012	G	T	0.07	T	synonymous_variant	LOW	T14E8.4	WBGene00043981	T14E8.4.1	protein_coding	c.738C>A	p.Ile246Ile
X	6561013	A	T	0.01	T	missense_variant	MODERATE	T14E8.4	WBGene00043981	T14E8.4.1	protein_coding	c.737T>A	p.Ile246Asn
X	6561030	C	T	0.54	T	synonymous_variant	LOW	T14E8.4	WBGene00043981	T14E8.4.1	protein_coding	c.720G>A	p.Thr240Thr
X	6561062	C	T	0	T	missense_variant	MODERATE	T14E8.4	WBGene00043981	T14E8.4.1	protein_coding	c.688G>A	p.Ala230Thr
X	6561122	T	A	0	A	missense_variant	MODERATE	T14E8.4	WBGene00043981	T14E8.4.1	protein_coding	c.628A>T	p.Ile210Phe
X	6561199	G	T	0.03	T	missense_variant	MODERATE	T14E8.4	WBGene00043981	T14E8.4.1	protein_coding	c.551C>A	p.Thr184Asn
X	6561201	T	A	0.02	A	missense_variant	MODERATE	T14E8.4	WBGene00043981	T14E8.4.1	protein_coding	c.549A>T	p.Leu183Phe
X	6561212	A	G	0	G	splice_region_variant&intron_variant	LOW	T14E8.4	WBGene00043981	T14E8.4.1	protein_coding	c.544-6T>C	NA
X	6561830	G	A	0	A	synonymous_variant	LOW	T14E8.4	WBGene00043981	T14E8.4.1	protein_coding	c.403C>T	p.Leu135Leu
X	6562016	G	C	0.01	C	missense_variant	MODERATE	T14E8.4	WBGene00043981	T14E8.4.1	protein_coding	c.217C>G	p.Gln73Glu
X	6562145	A	T	0	T	missense_variant	MODERATE	T14E8.4	WBGene00043981	T14E8.4.1	protein_coding	c.138T>A	p.Asn46Lys
X	6562349	A	T	0	T	missense_variant	MODERATE	T14E8.4	WBGene00043981	T14E8.4.1	protein_coding	c.18T>A	p.Phe6Leu
X	6562355	T	A	0.05	A	missense_variant	MODERATE	T14E8.4	WBGene00043981	T14E8.4.1	protein_coding	c.12A>T	p.Leu4Phe
X	6562361	C	G	0.01	G	missense_variant	MODERATE	T14E8.4	WBGene00043981	T14E8.4.1	protein_coding	c.6G>C	p.Arg2Ser

Figure S8: List of naturally occurring *aaim-1* variants in wild isolates of *C. elegans*.

This table represents a list of *T14E8.4* coding variants found to naturally occur in wild isolates of *C. elegans* generated by the CeNDR variant browser.[43] The reference allele (REF) as well as the alternate variant (ALT) and the allele frequency (AF) are displayed for various sites (POS) across *T14E8.4*. The nature (effect) and impact of these variants are depicted as well as the nucleotide changes (nt_change) and the corresponding amino acid change (aa_change). *T14E8.4* does not possess any variants predicted to have a high impact, implying that there are no obvious loss of function alleles and that its retention in the wild is advantageous.

869 **Supplemental table 1: List of strains utilized in this study**

Strain name	**Genotype**	**Source**
N2	Wild-type , Bristol strain	Caenorhabditis genetics center (CGC)
fawn-1 (AWR 05)	*aaim-1 (kea89)* X C127T , Q43Stop	This study
fawn-2 (AWR 11)	*aaim-1 (kea90)* X G221A splice site mutation	This study
fawn-3 (AWR 17)	*aaim-1 (kea28)* X 2.2 kb deletion	This study
fawn-4 (AWR03)	*aaim-1 (kea91)* X C1286T, A429V	This study
DM7448	VC20019 Ex[*Pmyo-3::YFP*])	Mok et al. (2020)[75]
RB563	*aaim-1 (ok295)* X	CGC
AWR 73	*aaim-1 (kea22)* X	This study
AWR 83	*aaim-1 (kea28)* X	This study
DA465	*eat-2 (ad465)* II	CGC
AWR 131	N2Ex[p*myo2::mCherry::Unc54,* p*aaim-1::GFP::3xFlag::Unc54]*	This study
AWR 125	*aaim-1 (kea28* Ex*[*p*myo2::mCherry::Unc54,* p*aaim-1::GFP::3xFlag::Unc54])*	This study
AWR 122	*aaim-1 (kea28* Ex*[*p*myo3::mCherry::Unc54,* p*aaim-1::GFP::Unc54])*	This study
AWR 115	*aaim-1 (kea28* Ex*[*p*myo2::mCherry::Unc54,* p*aaim-1::aaim-1::Unc54])*	This study

AWR119	*aaim-1 (kea28* Ex*[*p*myo2::mCherry::Unc54,* p*aaim-1::aaim-1*::3xFlag::*Unc54])*	This study
AWR 127	*aaim-1 (kea28*Ex*[*p*myo2::mCherry::Unc54,* p*aaim-1::SPΔ aaim-1::3xFlag::Unc54])*	This study
AWR129	*aaim-1 (kea28* Ex*[*p*myo2::mCherry::Unc54,* p*spp-5:: aaim-1::3xFlag::Unc54])*	This study
YY1446	*znfx-1*(*gg634[*HA::tagRFP::*znfx-1*]) II.	CGC

870

871

872

873

874

875

876

877

878

879

880

881

882

883

884

885

886 **Supplemental table 2: Spore doses utilized in this study.**

Species	**Dose**	**Plate concentration (spores/cm^2)**	**Total spores on assay plate (Millions) Plate size: *3.5cm, **6cm, ***10cm**
N. parisii	Very low	25,984	0.25*
	low	207,875	2.0*
	Medium-1	1,247,232	3.0*
	Medium-2	115,050	3.25
	Medium-2	41,380	3.25**
	Medium-3	141,600	4.0
	High	194,700	5.50
	Very high	318,600	9.0
	Maximal	637,200	18.0
N. ausubeli	Medium	103,936	1.0*
	High	519,680	5.0*

887

888

889

890

891

892

893

894

895

896 **Supplemental table 3: Primer sequences.**

Primer description	**Sequence**
Forward primer to amplify *aaim-1*	5'- atgaggttattatttttttcagcat -3'
Reverse primer to amplify *aaim-1*	5'-ttaatttttttgctggtgagg-3'
Forward primer to generate *SPΔaaim-1*	5'-atgctaaaggatttcttgccgtg-3'
Forward primer to amplify p*aaim-1*	5'-ttagtttggaaatgcacaaaaaaactgatctct-3'
Reverse primer to amplify p*aaim-1*	5-cagtggacttctgcttattaaaatgacttc-3'
Forward primer to amplify p*myo2*	5'-cattttatatctgagtagtatcctttgctttaaatgtcc-3'
Reverse primer to amplify p*myo2*	5'- gcatttctgtgtctgacgat-3'
Forward primer to amplify p*spp5*	5'-aaagcaaaatatcattatttgggaaaatc-3'
Reverse primer to amplify p*spp5*	5'-tctgtaataaaataaattgaaatgaaacac-3'
Forward primer to amplify GFP from pDD282	5'-atgagtaaaggagaagaattgttcact-3'
Reverse primer to amplify GFP from pDD282	5'-ttacttgtagagctcgtccattccg-3'
Forward ultramer to add a Gly Ala Gly Ser **linker** and 3x Flag with *stop codon* to C-Terminal end of constructs in **pDDONR221** via round the horn PCR.[67]	5'- **ggagccggatct**gattataaagacgatgacgataagcgtgactacaaggacgacgacgaca agcgtgattacaaggatgacgatgacaagaga*taa***acccagctttcttgtacaaagttg**-3'

897

898 **References:**

1. Murareanu Brandon M. *et al.* Generation of a Microsporidia Species Attribute Database and Analysis of the Extensive Ecological and Phenotypic Diversity of Microsporidia. *mBio* **0**, e01490-21.
2. Corradi, N. Microsporidia: Eukaryotic Intracellular Parasites Shaped by Gene Loss and Horizontal Gene Transfers. *Annu. Rev. Microbiol.* **69**, 167–183 (2015).
3. Wadi, L. & Reinke, A. W. Evolution of microsporidia: An extremely successful group of eukaryotic intracellular parasites. *PLoS Pathog.* **16**, e1008276 (2020).
4. Balla, K. M., Andersen, E. C., Kruglyak, L. & Troemel, E. R. A Wild C. Elegans Strain Has Enhanced Epithelial Immunity to a Natural Microsporidian Parasite. *PLOS Pathog.* **11**, e1004583 (2015).
5. Routtu, J. & Ebert, D. Genetic architecture of resistance in Daphnia hosts against two species of host-specific parasites. *Heredity* **114**, 241–248 (2015).
6. Martín-Hernández, R. *et al.* Nosema ceranae in Apis mellifera: a 12 years postdetection perspective. *Environ. Microbiol.* **20**, 1302–1329 (2018).
7. Jaroenlak, P. *et al.* Identification, characterization and heparin binding capacity of a spore-wall, virulence protein from the shrimp microsporidian, Enterocytozoon hepatopenaei (EHP). *Parasit. Vectors* **11**, 1–15 (2018).
8. Stentiford, G. D. *et al.* Microsporidia – Emergent Pathogens in the Global Food Chain. *Trends Parasitol.* **32**, 336–348 (2016).
9. Han, B. & Weiss, L. Therapeutic targets for the treatment of microsporidiosis in humans. *Expert Opin. Ther. Targets* **22**, (2018).

10. Han, B., Takvorian, P. M. & Weiss, L. M. Invasion of Host Cells by Microsporidia. *Front. Microbiol.* **11**, (2020).

11. Jarkass, H. T. E. & Reinke, A. W. The ins and outs of host-microsporidia interactions during invasion, proliferation and exit. *Cell. Microbiol.* **n/a**, e13247.

12. Hayman, J. R., Hayes, S. F., Amon, J. & Nash, T. E. Developmental Expression of Two Spore Wall Proteins during Maturation of the Microsporidian Encephalitozoon intestinalis. *Infect. Immun.* **69**, 7057–7066 (2001).

13. Hayman, J. R., Southern, T. R. & Nash, T. E. Role of Sulfated Glycans in Adherence of the Microsporidian Encephalitozoon intestinalis to Host Cells In Vitro. *Infect. Immun.* **73**, 841–848 (2005).

14. Southern, T. R., Jolly, C. E., Lester, M. E. & Hayman, J. R. EnP1, a Microsporidian Spore Wall Protein That Enables Spores To Adhere to and Infect Host Cells In Vitro. *Eukaryot. Cell* **6**, 1354–1362 (2007).

15. Li, Y. *et al.* Identification of a novel spore wall protein (SWP26) from microsporidia Nosema bombycis. *Int. J. Parasitol.* **39**, 391–398 (2009).

16. Wu, Z. *et al.* Proteomic analysis of spore wall proteins and identification of two spore wall proteins from Nosema bombycis (Microsporidia). *Proteomics* **8**, 2447–2461 (2008).

17. Chen, L., Li, R., You, Y., Zhang, K. & Zhang, L. A Novel Spore Wall Protein from Antonospora locustae (Microsporidia: Nosematidae) Contributes to Sporulation. *J. Eukaryot. Microbiol.* **64**, 779–791 (2017).

18. Xu, Y., Takvorian, P., Cali, A. & Weiss, L. M. Lectin Binding of the Major Polar Tube Protein (PTPl) and its Role in Invasion. *J. Eukaryot. Microbiol.* **50**, 600–601 (2003).

19. Xu, Y., Takvorian, P. M., Cali, A., Orr, G. & Weiss, L. M. Glycosylation of the Major Polar Tube Protein of Encephalitozoon hellem, a Microsporidian Parasite That Infects Humans. *Infect. Immun.* **72**, 6341–6350 (2004).

20. Han, B. *et al.* The role of microsporidian polar tube protein 4 (PTP4) in host cell infection. *PLOS Pathog.* **13**, e1006341 (2017).

21. Han, B. *et al.* Microsporidia Interact with Host Cell Mitochondria via Voltage-Dependent Anion Channels Using Sporoplasm Surface Protein 1. *mBio* **10**, (2019).

22. Luallen, R. J. *et al.* Discovery of a Natural Microsporidian Pathogen with a Broad Tissue Tropism in Caenorhabditis elegans. *PLoS Pathog.* **12**, e1005724 (2016).

23. Zhang, G. *et al.* A Large Collection of Novel Nematode-Infecting Microsporidia and Their Diverse Interactions with Caenorhabditis elegans and Other Related Nematodes. *PLOS Pathog.* **12**, e1006093 (2016).

24. Troemel, E. R., Félix, M.-A., Whiteman, N. K., Barrière, A. & Ausubel, F. M. Microsporidia Are Natural Intracellular Parasites of the Nematode Caenorhabditis elegans. *PLoS Biol.* **6**, e309 (2008).

25. Troemel, E. R. New Models of Microsporidiosis: Infections in Zebrafish, C. elegans, and Honey Bee. *PLOS Pathog.* **7**, e1001243 (2011).

26. Balla, K. M., Luallen, R. J., Bakowski, M. A. & Troemel, E. R. Cell-to-cell spread of microsporidia causes Caenorhabditis elegans organs to form syncytia. *Nat. Microbiol.* **1**, 16144 (2016).

27. Willis, A. R. *et al.* A parental transcriptional response to microsporidia infection induces inherited immunity in offspring. *Sci. Adv.* **7**, (2021).

28. Botts, M. R., Cohen, L. B., Probert, C. S., Wu, F. & Troemel, E. R. Microsporidia Intracellular Development Relies on Myc Interaction Network Transcription Factors in the Host. *G3 GenesGenomesGenetics* **6**, 2707–2716 (2016).

29. Szumowski, S. C., Botts, M. R., Popovich, J. J., Smelkinson, M. G. & Troemel, E. R. The small GTPase RAB-11 directs polarized exocytosis of the intracellular pathogen N. parisii for fecal-oral transmission from C. elegans. *Proc. Natl. Acad. Sci.* **111**, 8215–8220 (2014).

30. Balla, K. M., Lažetić, V. & Troemel, E. R. Natural variation in the roles of C. elegans autophagy components during microsporidia infection. *PLOS ONE* **14**, e0216011 (2019).

31. Reddy, K. C. *et al.* Antagonistic paralogs control a switch between growth and pathogen resistance in C. elegans. *PLoS Pathog.* **15**, e1007528 (2019).

32. Tecle, E. *et al.* The purine nucleoside phosphorylase pnp-1 regulates epithelial cell resistance to infection in C. elegans. *PLOS Pathog.* **17**, e1009350 (2021).

33. Luallen, R. J., Bakowski, M. A. & Troemel, E. R. Characterization of Microsporidia-Induced Developmental Arrest and a Transmembrane Leucine-Rich Repeat Protein in Caenorhabditis elegans. *PLOS ONE* **10**, e0124065 (2015).

34. Mok, C. A. *et al.* MIP-MAP: High-Throughput Mapping of Caenorhabditis elegans Temperature-Sensitive Mutants via Molecular Inversion Probes. *Genetics* **207**, 447–463 (2017).

35. Almagro Armenteros, J. J. *et al.* SignalP 5.0 improves signal peptide predictions using deep neural networks. *Nat. Biotechnol.* **37**, 420–423 (2019).

36. Reinke, A. W., Balla, K. M., Bennett, E. J. & Troemel, E. R. Identification of microsporidia host-exposed proteins reveals a repertoire of rapidly evolving proteins. *Nat. Commun.* **8**, 14023 (2017).

988 37. Ghafouri, S. & McGhee, J. D. Bacterial residence time in the intestine of Caenorhabditis
989 elegans. *Nematology* **9**, 87–91 (2007).
990 38. Engelmann, I. *et al.* A Comprehensive Analysis of Gene Expression Changes Provoked by
991 Bacterial and Fungal Infection in C. elegans. *PLoS ONE* **6**, e19055 (2011).
992 39. Head, B. P., Olaitan, A. O. & Aballay, A. Role of GATA transcription factor ELT-2 and p38
993 MAPK PMK-1 in recovery from acute *P. aeruginosa* infection in *C. elegans*. *Virulence* **8**,
994 261–274 (2017).
995 40. Styer, K. L. *et al.* Innate immunity in Caenorhabditis elegans is regulated by neurons
996 expressing NPR-1/GPCR. *Science* **322**, 460–464 (2008).
997 41. Tan, M. W., Mahajan-Miklos, S. & Ausubel, F. M. Killing of Caenorhabditis elegans by
998 Pseudomonas aeruginosa used to model mammalian bacterial pathogenesis. *Proc. Natl.*
999 *Acad. Sci. U. S. A.* **96**, 715–720 (1999).
1000 42. Kirienko, N. V., Cezairliyan, B. O., Ausubel, F. M. & Powell, J. R. Pseudomonas aeruginosa
1001 PA14 Pathogenesis in Caenorhabditis elegans. in *Pseudomonas Methods and Protocols* (eds.
1002 Filloux, A. & Ramos, J.-L.) 653–669 (Springer, 2014). doi:10.1007/978-1-4939-0473-0_50.
1003 43. Cook, D. E., Zdraljevic, S., Roberts, J. P. & Andersen, E. C. CeNDR, the *Caenorhabditis*
1004 *elegans* natural diversity resource. *Nucleic Acids Res.* **45**, D650–D657 (2017).
1005 44. Dierking, K., Yang, W. & Schulenburg, H. Antimicrobial effectors in the nematode
1006 Caenorhabditis elegans: an outgroup to the Arthropoda. *Philos. Trans. R. Soc. B Biol. Sci.*
1007 **371**, 20150299 (2016).
1008 45. Suh, J. & Hutter, H. A survey of putative secreted and transmembrane proteins encoded in
1009 the C. elegans genome. *BMC Genomics* **13**, 333 (2012).

1010 46. Gallotta, I. *et al.* Extracellular proteostasis prevents aggregation during pathogenic attack.
1011 *Nature* **584**, 410–414 (2020).
1012 47. Strzyz, P. Bend it like glycocalyx. *Nat. Rev. Mol. Cell Biol.* **20**, 388–388 (2019).
1013 48. Hoffman, C. L., Lalsiamthara, J. & Aballay, A. Host Mucin Is Exploited by Pseudomonas
1014 aeruginosa To Provide Monosaccharides Required for a Successful Infection. *mBio* **11**,
1015 (2020).
1016 49. Steentoft, C. *et al.* Precision mapping of the human O-GalNAc glycoproteome through
1017 SimpleCell technology. *EMBO J.* **32**, 1478–1488 (2013).
1018 50. Jensen, P. H., Kolarich, D. & Packer, N. H. Mucin-type O-glycosylation – putting the pieces
1019 together. *FEBS J.* **277**, 81–94 (2010).
1020 51. Tran, D. T. & Ten Hagen, K. G. Mucin-type O-Glycosylation during Development. *J. Biol.*
1021 *Chem.* **288**, 6921–6929 (2013).
1022 52. Schulenburg, H. & Felix, M.-A. The Natural Biotic Environment of Caenorhabditis elegans.
1023 *Genetics* **206**, 55–86 (2017).
1024 53. Samuel, B. S., Rowedder, H., Braendle, C., Félix, M.-A. & Ruvkun, G. Caenorhabditis
1025 elegans responses to bacteria from its natural habitats. *Proc. Natl. Acad. Sci.* **113**, E3941–
1026 E3949 (2016).
1027 54. Sinha, A., Rae, R., Iatsenko, I. & Sommer, R. J. System Wide Analysis of the Evolution of
1028 Innate Immunity in the Nematode Model Species Caenorhabditis elegans and Pristionchus
1029 pacificus. *PLOS ONE* **7**, e44255 (2012).
1030 55. Ashe, A. *et al.* A deletion polymorphism in the Caenorhabditis elegans RIG-I homolog
1031 disables viral RNA dicing and antiviral immunity. *eLife* **2**, e00994 (2013).

1032 56. Reddy, K. C. *et al.* An Intracellular Pathogen Response Pathway Promotes Proteostasis in
1033 C. elegans. *Curr. Biol. CB* **27**, 3544-3553.e5 (2017).
1034 57. Toor, J. & Best, A. Evolution of Host Defense against Multiple Enemy Populations. *Am. Nat.*
1035 **187**, 308–319 (2016).
1036 58. Thaler, J. S., Fidantsef, A. L., Duffey, S. S. & Bostock, R. M. Trade-Offs in Plant Defense
1037 Against Pathogens and Herbivores: A Field Demonstration of Chemical Elicitors of Induced
1038 Resistance. *J. Chem. Ecol.* **25**, 1597–1609 (1999).
1039 59. Thompson, O. *et al.* The million mutation project: a new approach to genetics in
1040 Caenorhabditis elegans. *Genome Res.* **23**, 1749–1762 (2013).
1041 60. Bolger, A. M., Lohse, M. & Usadel, B. Trimmomatic: a flexible trimmer for Illumina
1042 sequence data. *Bioinforma. Oxf. Engl.* **30**, 2114–2120 (2014).
1043 61. Li, H. & Durbin, R. Fast and accurate short read alignment with Burrows-Wheeler transform.
1044 *Bioinforma. Oxf. Engl.* **25**, 1754–1760 (2009).
1045 62. DePristo, M. A. *et al.* A framework for variation discovery and genotyping using next-
1046 generation DNA sequencing data. *Nat. Genet.* **43**, 491–498 (2011).
1047 63. Wang, K., Li, M. & Hakonarson, H. ANNOVAR: functional annotation of genetic variants
1048 from high-throughput sequencing data. *Nucleic Acids Res.* **38**, e164 (2010).
1049 64. Schindelin, J. *et al.* Fiji: an open-source platform for biological-image analysis. *Nat. Methods*
1050 **9**, 676–682 (2012).
1051 65. Walhout, A. J. *et al.* GATEWAY recombinational cloning: application to the cloning of large
1052 numbers of open reading frames or ORFeomes. *Methods Enzymol.* **328**, 575–592 (2000).
1053 66. Hartley, J. L., Temple, G. F. & Brasch, M. A. DNA cloning using in vitro site-specific
1054 recombination. *Genome Res.* **10**, 1788–1795 (2000).

1055 67. Moore, S. D. & Prevelige, P. E. A P22 scaffold protein mutation increases the robustness of
1056 head assembly in the presence of excess portal protein. *J. Virol.* **76**, 10245–10255 (2002).
1057 68. Almagro Armenteros, J. J. *et al.* SignalP 5.0 improves signal peptide predictions using deep
1058 neural networks. *Nat. Biotechnol.* **37**, 420–423 (2019).
1059 69. Dokshin, G. A., Ghanta, K. S., Piscopo, K. M. & Mello, C. C. Robust Genome Editing with
1060 Short Single-Stranded and Long, Partially Single-Stranded DNA Donors in Caenorhabditis
1061 elegans. *Genetics* **210**, 781–787 (2018).
1062 70. Concordet, J.-P. & Haeussler, M. CRISPOR: intuitive guide selection for CRISPR/Cas9
1063 genome editing experiments and screens. *Nucleic Acids Res.* **46**, W242–W245 (2018).
1064 71. Amrit, F. R. G., Ratnappan, R., Keith, S. A. & Ghazi, A. The C. elegans lifespan assay
1065 toolkit. *Methods* **68**, 465–475 (2014).
1066 72. Crittenden, S. & Kimble, J. Preparation and Immunolabeling of Caenorhabditis elegans.
1067 *Cold Spring Harb. Protoc.* **2009**, pdb.prot5216-pdb.prot5216 (2009).
1068 73. Wan, G. *et al.* Spatiotemporal regulation of liquid-like condensates in epigenetic inheritance.
1069 *Nature* **557**, 679–683 (2018).
1070 74. Large-Scale Screening for Targeted Knockouts in the Caenorhabditis elegans Genome. *G3*
1071 *GenesGenomesGenetics* **2**, 1415–1425 (2012).
1072 75. Mok, C., Belmarez, G., Edgley, M. L., Moerman, D. G. & Waterston, R. H. PhenoMIP:
1073 High-Throughput Phenotyping of Diverse *Caenorhabditis elegans* Populations via Molecular
1074 Inversion Probes. *G3 GenesGenomesGenetics* **10**, 3977–3990 (2020).
1075